DANMARKS OG GRØNLANDS GEOLOGISKE UNDERSØGELSE RAPPORT 2019/23

Diagenesis modelling of the geothermal reservoir quality of the Gassum Formation sandstones

Mette Olivarius, Joachim Tremosa, Anders Mathiesen,
Rikke Weibel, Margrethe Thorup Dalgaard &
Lars Henrik Nielsen

GEOLOGICAL SURVEY OF DENMARK AND GREENLAND
DANISH MINISTRY OF CLIMATE, ENERGY AND UTILITIES

G E U S

DANMARKS OG GRØNLANDS GEOLOGISKE UNDERSØGELSE RAPPORT 2019/23

Diagenesis modelling of the geothermal reservoir quality of the Gassum Formation sandstones

GEOTHERM – Geothermal energy from sedimentary reservoirs – Removing obstacles for large scale utilization

Innovation Fund Denmark: project 6154-00011B
(Final report in WP3)

Mette Olivarius, Joachim Tremosa, Anders Mathiesen,
Rikke Weibel, Margrethe Thorup Dalgaard &
Lars Henrik Nielsen

GEOLOGICAL SURVEY OF DENMARK AND GREENLAND
DANISH MINISTRY OF CLIMATE, ENERGY AND UTILITIES

G E U S

Content

Dansk resumé 4

Executive abstract 6

1. Introduction 7

2. Geological setting 9

3. Samples and methods 10

4. Results 17

5. Prediction 40

6. Conclusions 52

Further studies 54

Acknowledgements 55

References 56

Dansk resumé

Den danske undergrund rummer sandstensreservoirer, der er velegnede til indvinding af geotermisk energi i store dele af landet. Potentialet er stort, men der er en række udfordringer forbundet med efterforskningen, hvoraf estimering af reservoirkvaliteten er en af de væsentligste, hvilket belyses i denne GEOTHERM rapport. Sandstenene i Gassum Formationen er begravet ved forskellige dybder i de forskellige områder i landet og har tidligere været begravet endnu dybere end i dag, så de mineralogiske omdannelser, der accelererer med stigende temperatur, har haft betydelig indflydelse på især de dybest liggende dele af reservoiret. Den nuværende begravelsesdybde er således ikke en direkte indikator for hvor fremskreden diagenesen er. Ud over den temperaturhistorie reservoiret har gennemgået har også den oprindeligt aflejrede mineralogiske sammensætning indflydelse på, hvilke diagenetiske forandringer der er sket under begravelsen, så det oprindelige aflejringsmiljø skal også tages i betragtning ved estimering af reservoirkvaliteten.

Den etablerede bassinmodel er kalibreret via organiske og mineralogiske temperaturindikatorer så den differentierede begravelseshistorie kan estimeres for hvert område. De tre typer diagenetiske omdannelser der er kritiske for reservoirkvaliteten af Gassum Formationens sandsten omfatter udfældning af kvarts-, ler- og karbonat-cement, der hver især kan mindske porøsiteten og permeabiliteten så meget, at geotermisk udvinding ikke er mulig. De mineralogiske ændringer, der er sket i sandstenene og deres indflydelse på reservoiregenskaberne, er derfor vurderet ved modellering af de diagenetiske processer. Det fremgår heraf at de forskellige cement-typer udfældes ved forskellige betingelser. Data fra en af de dybe boringer er blevet udeladt fra modellen og brugt til at validere modellens anvendelighed ved sammenligning mellem de målte værdier og de beregnede. Modellering af den mekaniske kompaktion, der hovedsagelig sker under den første del af begravelsen, er også inkluderet.

Resultaterne viser, at det er muligt at beregne cementmængder og reservoiregenskaber, der svarer til de målte, dog underestimeres yderpunkterne til en vis grad både hvad angår lave og høje værdier. Forskellige scenarier er beregnet for sandsten fra de forskellige aflejringsmiljøer, formationen blev dannet i, da deres diagenetiske udvikling er forskellig. På denne måde kan den seismiske dybdekortlægning af formationen sammenholdt med viden om temperaturudviklingen og fordelingen af aflejringsmiljøerne bruges til at beregne omfanget og karakteren af de diagenetiske processer og dermed reservoirkvaliteten for områder, hvor Gassum Formation udgør et potentielt geotermisk reservoir. Disse resultater er derfor meget lovende, idet modellen muliggør en kvantitativ vurdering af Gassum reservoirets kvalitet i geotermiske licenser før en boring udføres.

På denne baggrund anbefales det, at tilsvarende diagenesemodeller opstilles for de øvrige kendte sandstensformationer. Endvidere anbefales det at anvende resultaterne til at beregne den rumlige fordeling af reservoiregenskaber for reservoirernes samlede udbredelse via den seismiske kortlægning ved at tage temperatur- og facies-afhængigheden af de diagenetiske processer i betragtning.

Executive summary

Diagenesis modelling of the geothermal reservoirs onshore Denmark was initiated because the effects of mechanical compaction and diagenesis on the porosity and permeability vary much across the area due to differential burial histories and mineralogical compositions. Hence, an integrated approach is necessary to estimate the reservoir quality, and the Gassum Formation is used to test the applicability of the modelling approaches. Results of organic and mineralogical temperature constrains such as vitrinite reflectance, fluid inclusions in quartz cement and oxygen isotopes in carbonate cement are used to calibrate the basin modelling using the PetroMod software, and comparable results are obtained for the different input parameters.

Thermodynamic modelling of the mineralogical reactions by SURP provides important knowledge about the conditions for dissolution and precipitation of carbonate minerals, which result in low reservoir quality when they form pervasive cementations. The Mg availability in the pore water is triggering for when ankerite can precipitate, and the largest amounts are able to form when both calcite and siderite are available for dissolution. Integration of petrographic observations, mineralogical compositions, reservoir properties, depositional environments and burial histories in the calibration of compaction and diagenesis modelling by Touchstone produces reliable results as compared with test samples and analog data. The calculated quartz cement volumes correlate acceptably with the measured values, showing the reliability of the modelled burial histories since the quartz formation is strongly dependent on the temperature evolution.

The initial mineralogical composition and grain size varies in relation to depositional environments and source areas, so individual model scenarios take each of these settings into account to obtain a detailed estimate of the reservoir properties. In this way, a robust model for estimation of geothermal reservoir quality of the Gassum Formation has been establish, which can be used to make qualified pre-drill predictions on the basis of knowledge about the burial history and depositional setting. The establishment of corresponding models for the other geothermal reservoirs is recommended as well as using the existing seismic mapping to extend the estimated reservoir properties to obtain their spatial distribution by considering the temperature- and facies-dependence of the diagenetic processes.

1. Introduction

This study is funded by Innovation Fund Denmark and forms part of GEOTHERM – Geothermal energy from sedimentary reservoirs – Removing obstacles for large scale utilization, project 6154-00011B. The report finalizes the reporting of Milestone 3.6a in Work Package 3. The diagenesis modelling was initiated in order to enable estimation of crucial reservoir properties prior to costly drilling in geothermal exploration licenses. Sufficiently large porosities and permeabilities are required for efficient geothermal water flow and both parameters vary much in the Gassum Formation related to the burial and temperature history and the initial mineralogy, which is mainly determined by the depositional environments and the bedrock in the hinterland (Nielsen 2003, Kristensen et al. 2016, Weibel et al. 2017a, Weibel et al. 2017b).

Modelling of reservoir quality has been applied to hydrocarbon reservoirs where the Touchstone modelling tool has proven useful (e.g. Tobin et al. 2010, Ajdukiewicz et al. 2010, Taylor et al. 2015, English et al. 2017, Busch et al. 2018). However, reservoir quality modelling has not been applied for the purpose of geothermal energy exploitation before. A combined modelling approach is applied in this study because several controversies within reservoir quality prediction still exist and not all mineral reactions are well understood (e.g. Taylor et al. 2010, Cui et al. 2017, Worden et al. 2018). Hence, the rigorous compaction and silicate models in Touchstone are calibrated to the Danish area and new knowledge about the evolution in carbonate cement type and amount is obtained by SURP modelling in relation to the pore-water composition, since the carbonate cements may be equally important for the reservoir quality. SURP has successfully been applied to mudstones (Tremosa et al. 2020) and is further developed for sandstones during the GEOTHERM project considering the diagenetic evolution of the Gassum Formation.

By using basin modelling to study the thermal and structural evolution, it is possible to quantify the geological history for example by assessing phases of uplift and erosion. Basin modelling is especially relevant in areas affected by burial anomalies and with past maximum burial depths that exceeds present-day burial, such that differences in temperature, porosity and permeability are evident when calculating scenarios with and without considering uplift and erosion. Thus, detailed knowledge of eroded thicknesses and the influence of the erosion on the geological framework is important for predicting the porosity and permeability in sandstones and mudstones. Estimation and related uncertainties of these parameters, especially in a more regional context, are essential for successful exploration of geothermal energy.

Quantification and modelling of burial, maturity and temperature histories are the major goals of the basin modelling, allowing for a better understanding of the general geological evolution within the Danish onshore area where the Gassum Formation is widely distributed and mostly in depths and thicknesses appropriate for geothermal energy (Fig. 1.1). The area has undergone at least one phase of inversion and must therefore have experienced moderate to high amounts of erosion, hence decreasing the influence of diagenesis following the structural inversion. The aim of the study is to reconstruct the compaction and diagenesis histories and the resulting evolution in reservoir properties of the studied sandstones such that the reservoir quality of the Gassum Formation can be predicted in areas where only the burial history is given by e.g. seismic data.

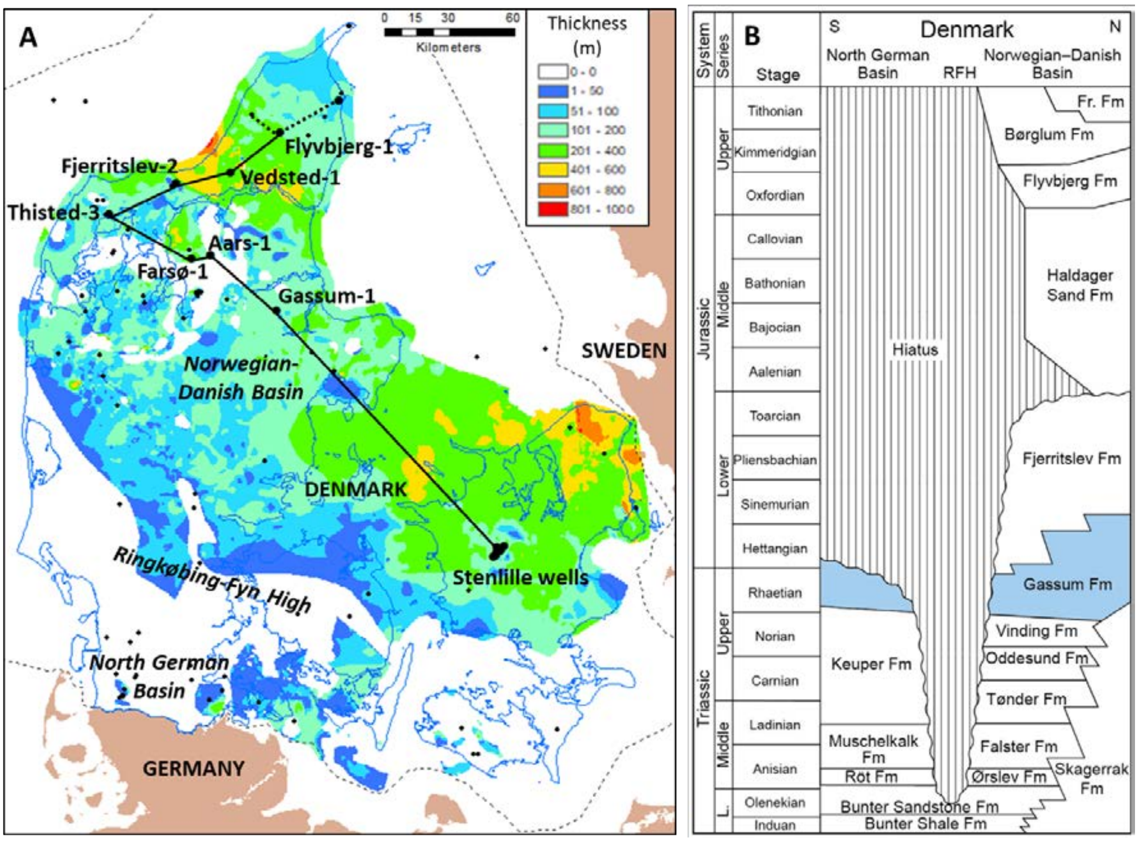

Figure 1.1: *A. Seismic thickness map of the Gassum Formation in the eastern part of the Norwegian–Danish Basin with locations of the wells applied in this study. B. Stratigraphic scheme based on Michelsen and Clausen (2002) and Nielsen (2003). RFH: Ringkøbing–Fyn High. Fr. Fm: Frederikshavn Formation.*

2. Geological setting

Crustal stretching followed by late Carboniferous–early Permian rifting and Mesozoic–Cenozoic thermal-dominated subsidence resulted in the formation of the Norwegian-Danish Basin (Vejbæk 1997). The thick succession of sandstones, siltstones, mudstones, carbonates and evaporites in the basin includes a number of potential geothermal reservoir rocks. Especially the sandstones in the Triassic–Jurassic succession are suitable for this purpose, including the Bunter Sandstone Formation, the Skagerrak Formation, the Gassum Formation, the Haldager Sand Formation and the Frederikshavn Formation (Fig. 1.1B).

The Upper Triassic–Lower Jurassic Gassum Formation sandstones are appropriate for geothermal exploitation in many areas onshore Denmark as evident by the temperature distribution, mineralogical composition, formation water chemistry and reservoir properties (Fuchs et al. 2020, Holmslykke et al. 2019, Kristensen et al. 2016, Mathiesen et al. 2010, Poulsen et al. 2017, Vosgerau et al. 2016, Weibel et al. 2017a, Weibel et al. 2017b).

The Gassum Formation is present in most of the Norwegian–Danish Basin, except on the Ringkøbing–Fyn High and where major salt structures are present (Fig. 1.1A) (Michelsen et al. 2003, Nielsen 2003). The formation was deposited during humid climatic conditions and consists of fluvial, estuarine, lagoonal and shoreface sandstones interbedded with marine and lacustrine mudstones, siltstones and thin coal beds formed in response to sea-level fluctuations (Fig. 2.1).

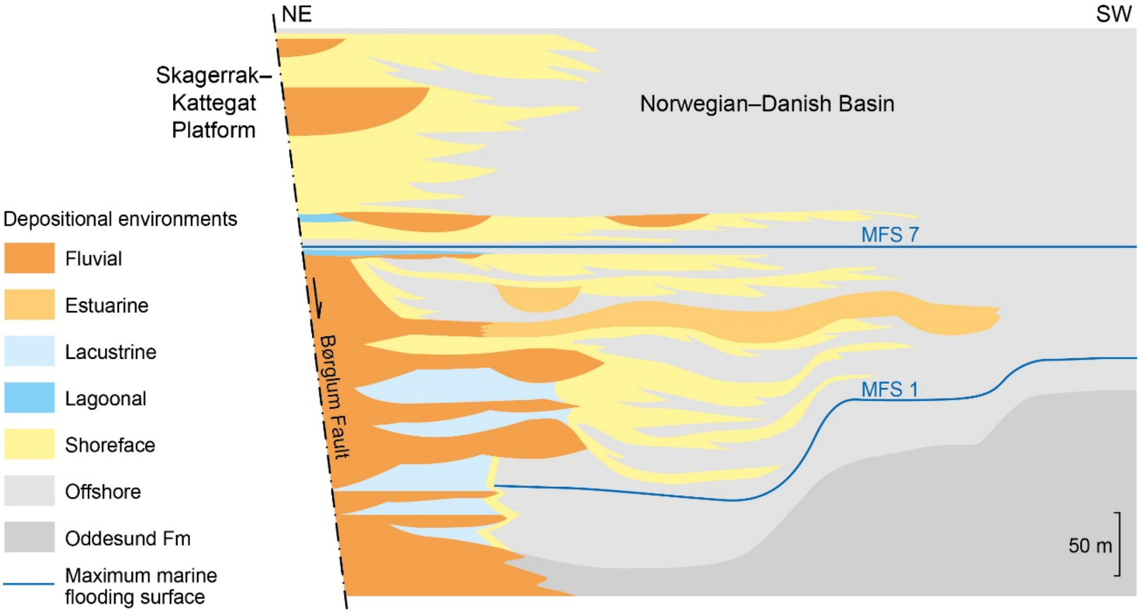

Figure 2.1: *Schematic cross-section of the general development of depositional environments across the Norwegian–Danish Basin. From Weibel et al. (2017a).*

3. Samples and methods

The studied sandstones are from present-day burial depths of c. 1170–3360 m corresponding to estimated maximum burial depths of c. 1670–3860 m prior to the structural inversion during Neogene time. This large depth variation is related to the differential subsidence experienced in the different parts of the basin. The studied samples are from the Aars-1, Farsø-1, Fjerritslev-2, Flyvbjerg-1, Gassum-1, Stenlille-15, -18, -19, Thisted-3 and Vedsted-1 wells (Figs 1.1, 3.1).

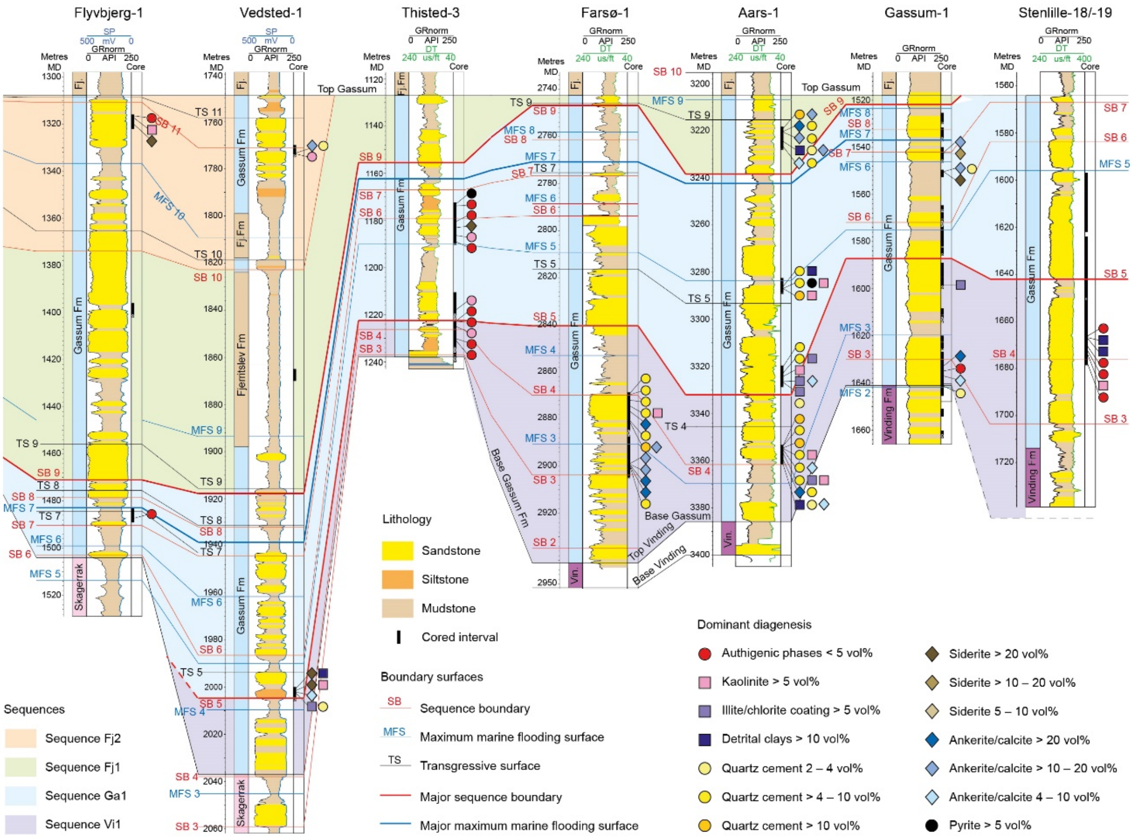

Figure 3.1: *Log panel from Weibel et al. (2017a) with sequence stratigraphic interpretations from Nielsen (2003). The dominant diagenetic alteration is shown with a symbol for each sample. The Fjerritslev-2 well is not included since the well logs are of too poor quality. The location of the well-log profile is drawn in Figure 1.1.*

3.1 Petrography

Polished thin sections with blue epoxy were produced for 78 samples and K-feldspar staining was made on half of each thin section. Petrographic point counting of 500 minerals plus porosity was performed for each thin section by optical microscopy, and the resulting modal compositions of the sandstones are in volume percentage. The grain size and sorting were calculated from thin-section measurements. Further studies of the paragenetic relationships and mineral chemistries were made on gold-coated rock chips and carbon-coated thin sections using a Phillips XL 40 scanning electron microscope (SEM) equipped with an energy dispersive X-ray (EDS) detector. Microprobe analyses of the composition of carbonate minerals were performed at University of Copenhagen.

3.2 Core analysis

Core analysis including porosity, permeability and grain density measurements was performed in accordance with the API RP-40 standard (American Petroleum Institute 1998) on 71 horizontal core plugs for which the end-cuts were used for the petrographic investigations. For three of the samples, the permeability could not be measured since these core plugs were damaged during the measurement. The He-porosities were measured at unconfined conditions, and the gas permeabilities were measured at a confining pressure of 2.8 MPa and a mean N_2 gas pressure of c. 0.15 MPa. The samples were cleaned in methanol prior to analysis to remove NaCl.

Overburden measurements of a subset of five samples were performed at 25°C and at increasing confining pressure with analysis of porosity and fluid permeability at 10, 39, 100, 200 and 300 bar. These hydrostatic stress analyses were made to test if porosity and permeability are considerably lower in the reservoir compared to surface conditions, which must be considered when estimating the reservoir quality.

3.3 Fluid inclusions

The fluid inclusion microthermometry was performed on a Leica microscope with a 100x objective and a camera coupled to a Linkam THMSG 600 heating-freezing stage to obtain information about the homogenization temperatures of fluid inclusions trapped in quartz cement. The fluid inclusions in the Gassum Formation are very small so analysis was only possible in three samples from the deepest wells where the inclusions are slightly larger.

3.4 Stable isotopes

Secondary ion mass spectrometry (SIMS) stable isotope analyses of carbonate cement in thin sections were carried out at a CAMECA IMS 1280 ion microprobe at the Nordsim laboratory at the Swedish Museum of Natural History, Stockholm, Sweden. The analyses were performed on fragments of thin sections mounted in epoxy and coated with gold. The beam size was ~ 10 µm for $\delta^{18}O$ and ~ 15 µm $\delta^{13}C$. Each run was initiated with two standards and proceeded with one standard per 6 sample runs. The standards were used to provide an external precision on the analyses and to correct for instrumental mass bias and minor drift in the instrument. Each individual analysis comprised a pre-sputter to remove gold coating, beam centering and 64s of data acquisition. $\delta^{18}O$ and $\delta^{13}C$ isotopic values for carbonates are reported relative to V-PDB. $\delta^{18}O$ isotopic values for quartz are reported relative to SMOW.

The calcite standard S0161, which comes from a granulite facies marble in the Adirondack Mountains, was kindly provided by R.A. Stern, University of Alberta. The values used for corrections for instrumental mass fractionation were determined by conventional stable isotope mass spectrometry at Stockholm University, with ten separate aliquots yielding $\delta^{13}C_{PDB}$ = -0.22 ± 0.11 ‰ (1 std. dev.), $\delta^{18}O_{PDB}$ = -5.62 ± 0.11 ‰ (1 std. dev.) and $\delta^{18}O_{VSMOW}$ = 25.12 ± 0.12 ‰ (1 std. dev.). The ankerite standard from Eisenerz, Styria, Austria, has a reported $\delta^{18}O_{VSMOW}$ = 15.99 ± 0.51 ‰ (2 std. dev.) for Fe/(Mg+Fe) = 0.789 (Sliwinski et al. 2015). The oxygen and carbon isotope composition of the carbonates ($\delta^{18}O$ and $\delta^{13}C$) are reported as per mil (‰) deviations of the isotope ratios ($^{18}O/^{16}O$ and $^{13}C/^{12}C$) calculated to the V-PDB scale.

3.5 Basin maturity model

Basin maturity modelling is used as a tool for integration of a wide range of geological, geophysical, geochemical and petrophysical data and serves as a framework for testing numerous hypotheses concerning origin and evolution of the basin, the processes herein and the geological development of its petroleum resources. The object of the basin modelling is originally to investigate thermal maturity of the potential source rock, as timing and extent of source rock maturation is crucial to understand petroleum systems (e.g. Magoon and Dow 1994). The aim of applying the basin modelling in the GEOTHERM study is primary to deliver input parameters for the diagenesis modelling with Touchstone and SURP. After using this approach to further constrain the calibrated forward diagenesis modelling, the estimated temporal and spatial distribution of reservoir properties can be used to guide the selection of lithofacies input to future basin modelling.

Basin maturity modelling is in this study conducted using the 1D PetroMod (IES®, Integrated Exploration Systems GmbH, Aachen, Germany, v2018.1) software on eight wells all situated within the Danish onshore area (Fig. 1.1) by using re-evaluated and newly analysed vitrinite reflectance and temperature data. A mutual basin modelling is performed for the three Stenlille wells. The aim of the 1D basin modelling is to organize and integrate the knowledge of the geological development in order to establish a conceptual model that contains all the key elements, which can then deliver input data for the Touchstone and SURP modelling tools comprising burial history, temperature history, effective stress history and overpressure history.

3.6 Diagenesis models

3.6.1 Presentation of the SURP code

The SURP code is under development at BRGM to account for both thermo-hydro-mechanical and mineralogical effects and their reciprocal influence during the burial of a 1D sedimentary pile (Tremosa et al. 2020). It includes the influence of temperature and pressure evolution on mineralogical diagenetic reactions and the influence of porosity variations by mineralogical precipitation and dissolution, the fluid pressure and the effective stress in the sedimentary pile. The SURP code consists of a coupling between the thermo-hydro-mechanical calculations, made using a Python code source, and the IPHREEQC geochemical calculation code (Charlton and Parkhurst 2011) used for the thermodynamic and mineralogical calculations. The mineral evolution is calculated assuming a thermodynamic equilibrium between the pore water and the mineral assemblage forming the rock. The calculated diagenetic evolution is then driven by the temperature changes but also depends on the pore water composition. During the sediment burial, the porosity evolves both because of the mechanical compaction of the rock and because of the mineral precipitations and dissolutions. It is then possible to distinguish the individual effects of compaction and diagenesis on porosity evolution.

3.6.2 Establishment of burial model

The model grid was established from the lithological layers used in the PetroMod burial model and their thickness at the time of deposition, calculated by a back-stripping approach. The sedimentary piles were described as a 1D geometry by 59 grid cells at Stenlille, 79 grid cells at Vedsted, 98 grid cells at Farsø and 105 grid cells at Aars of variable size ranging from 4 to 105 m, including a grid-size refinement in the target Gassum Formation. A lithology description (sandstone, shaly sandstone, shale or chalk) and corresponding mechanical, hydraulic and mineralogical property parameters were assigned to each lithological layer. The sedimentation rate and its evolution over time was obtained from the thickness and the age of each lithological layer.

The sediments are successively simulated to deposit according to the sedimentation rate and are progressively buried. Because of the weight of the overlying sediments, the sediments are compacted leading to a porosity decrease (Tremosa et al. 2020). In accordance with the porosity decrease, the sediment thickness also decreases in order to correspond to the present-day thickness at the end of the simulation when considering an absence of the Neogene uplift event. Temperature increases with the sediment burial depth following a geothermal gradient of 27°C/km that remains constant during the simulation.

3.6.3 Diagenesis calculation parameters

The SURP code offers the possibility to calculate the evolution of a mineralogical assemblage during the burial of a sediment pile, driven by the temperature increase with depth. Selected primary mineral phases were simulated to dissolve while a thermodynamic equilibrium was considered between the mineralogical assemblage and the pore water, which evolved in the simulation from dilute water to the formation water composition by Holmslykke et al. (2019).

Selection of mineral phases involved in the calculations was constrained by the diagenetic sequence determined by the petrographic investigations. Primary minerals that were observed to dissolve comprise micas and feldspars and were considered in the model as biotite, phlogopite, microcline and albite, dissolving in proportions of 6.0, 0.1, 1.0 and 0.1, respectively. Diagenetic constraints on precipitating phases include that quartz starts to precipitate at about 2 km depth in amounts that increase with depth; kaolinite precipitates very early; illite precipitates mainly at depth; chlorite precipitates in small amount and is restricted to estuarine and shoreface sandstones deposited during forced regressive conditions. Regarding the carbonate minerals, calcite and siderite dissolve during burial and are replaced by ankerite. In the reactive model, quartz, kaolinite, chlorite, illite and ankerite were allowed to precipitate at local thermodynamic equilibrium, while calcite and siderite can dissolve or precipitate at thermodynamic equilibrium. Composition and thermodynamic parameters of the mineral phases involved in the SURP modelling are reported in Table 3.1.

Increasing pore-water salinity with depth is considered in the model, reaching the formation water composition at maximum burial depth. The employed initial pore-water composition corresponds to the formation water diluted 100 times, which evolves during the simulation to reach the formation water composition with salinities ranging between 3.5 and 6.4 mol/L (170 to 300 g/L) in the different wells where the Gassum Formation water has been sampled and analyzed.

The porosity evolves both because of sediment compaction due to the weight of the overlying sediments and because of diagenetic reactions. The porosity variations caused by sediment compaction are driven by the evolution of the effective stress depending on compaction parameters determined for each lithology type (Tremosa et al. 2020). The variations of volume induced by precipitating mineral phases are added to the porosity evolution.

Table 3.1: *Selection of mineral phases used in the SURP diagenetic model.*

Illite(Mg)	
K0.85Mg0.25Al2.35Si3.4O10(OH)2 + 8.4H+ + 1.6H2O = 2.35Al+3 + 0.85K+ + 0.25Mg+2 + 3.4H4SiO4	
log_K	*8.5*
delta_h	*-225.651*
Kaolinite	
Al2Si2O5(OH)4 + 6H+ = 2Al+3 + 2H4SiO4 + 1H2O	
log_K	*10*
delta_h	*-169.718*
Chlorite(Cca-2)	
(Mg2.964Fe1.927Al1.116Ca0.011)(Si2.633Al1.367)O10(OH)8 + 17.468H+ = 2.483Al+3 + 0.011Ca+2 + 1.712Fe+2 + 2.964Mg+2 + 2.633H4SiO4 + 0.215Fe+3 + 7.468H2O	
log_K	*61.315*
delta_h	*-612.127*
Quartz(alpha)	
SiO2 + 2H2O = H4SiO4	
log_K	*-9.5*
delta_h	*21.166*
Calcite	
CaCO3 + H+ = HCO3- + Ca+2	
log_K	*1.847*
delta_h	*-25.325*
Siderite	
FeCO3 + H+ = HCO3- + Fe+2	
log_K	*-0.273*
delta_h	*-27.862*
Ankerite	
CaMg0.3Fe0.7(CO3)2 + 2H+ = Ca+2 + 0.3Mg+2 + 0.7Fe+2 + 2HCO3-	
log_K	*1.54*
delta_h	
Muscovite(disordered)	
KAl2(AlSi3)O10(OH)2 + 10H+ = 3Al+3 + K+ + 3H4SiO4	
log_K	*14*
delta_h	*-276.123*
Phlogopite	
KMg3(AlSi3)O10(OH)2 + 10H+ = Al+3 + K+ + 3Mg+2 + 3H4SiO4	
log_K	*41.082*
delta_h	*-360.123*
Albite(low)	
NaAlSi3O8 + 4.000H+ + 4.000H2O = 1.000Al+3 + 1.000Na+ + 3.000H4SiO4	
log_K	*2.996*
delta_h	*-84.003*
Microcline	
K(AlSi3)O8 + 4H+ + 4H2O = Al+3 + K+ + 3H4SiO4	
log_K	*0.004*
delta_h	*-56.203*

3.6.4 Presentation of the Touchstone model

Petrography, reservoir properties and burial history data of the studied sandstones were analyzed by the software Touchstone™ developed by Geocosm LCC to make forward diagenesis modelling of the evolution in reservoir quality. The petrographic input data comprise the composition of detrital and authigenic phases, the grain-coat coverage and the grain size. The reservoir property data include unstressed porosity, permeability and density measurements besides a subset of stressed analyses. The burial history data comprise the evolution in depth, temperature and effective stress.

For each sample with petrographical data, the diagenetic development and reservoir properties are simulated in relation to the temperature and effective stress histories. The sensitivity of the model parameters is tested, and optimization of the parameters is made to find the best fit to the input data. When an acceptable match is obtained, then the model can be used to estimate the reservoir properties in areas without well control. The compositional variability is simulated and the uncertainty in the burial histories is tested to make the best possible estimation of the reservoir quality at the target locations.

4. Results

4.1 Reservoir characteristics

The Gassum Formation consists of sandstone layers interbedded with marine mudstone layers (Figs 2.1, 3.1) (Nielsen 2003). In this study, the sandstones are grouped into four depositional environment categories comprising fluvial, estuarine, lagoonal and shoreface. The estuarine category consists of estuarine-fluvial and tidal channel deposits, whereas lagoonal tidal creeks are included in the lagoonal category. The shoreface category comprises beach, foreshore, upper shoreface and lower shoreface to offshore depositional environments.

The sandstones in the Gassum Formation are mostly arkosic and subarkosic besides fewer quartzarenites and lithic subarkoses according to the definitions by McBride (1963). The fluvial sandstones have the largest feldspar content along with some of the shoreface sandstones, and a group of estuarine sandstones has the highest quartz content because these samples are from the easternmost part of the Norwegian–Danish Basin where the Gassum Formation sandstones in general have a high mineralogical maturity (Fig. 4.1). The studied sediments are very well to very poorly sorted and consist of very fine- to coarse-grained sandstones besides some siltstones (Weibel et al. 2017a). In general, increasing grain size correlates with decreasing sorting (Fig. 4.2). There is a general basinwards trend of decreasing grain size and increasing sorting.

The petrographic data are summarized in Table 4.1 for each of the wells applied in this study. The detrital grains are dominated by quartz comprising 33–77% of the sandstones and consisting of both monocrystalline quartz (average: 45%) and polycrystalline quartz (average: 6%). Feldspar grains are abundant in most samples, comprising 1–36% of the sandstones and consisting of albite-plagioclase (average: 9%) and K-feldspar (average: 6%). Especially the fluvial sandstones and some of the shoreface sandstones have high plagioclase abundances (Fig. 4.3). Lithic grains are present in amounts of 0–7% (Fig. 4.1), comprising sedimentary, metamorphic, plutonic and volcanic rock fragments in decreasing order of abundance. Mica grains include mostly muscovite and biotite, each present in average amounts of 1%. Heavy minerals, glauconite, carbonate fossils and organic matter are present in small amounts (average: <1%, maximum: <14%). The heavy mineral grains consist mostly of zircon, tourmaline and Fe-Ti-oxides. The glauconite is present in 15% of the samples, mainly from the shoreface category. The detrital clays comprise 0–21% of the samples and consist mostly of clay matrix besides some infiltration clays.

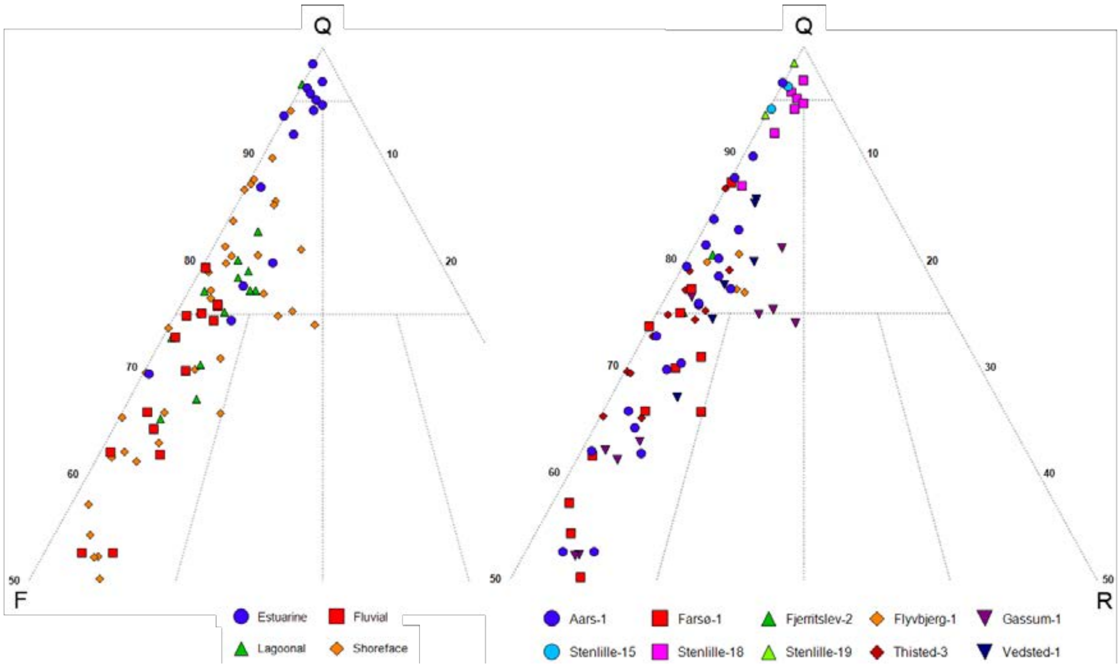

Figure 4.1: *QFR plot showing the relative proportions between quartz, feldspars and rock fragments based on the petrographic data grouped by depositional environments and by wells.*

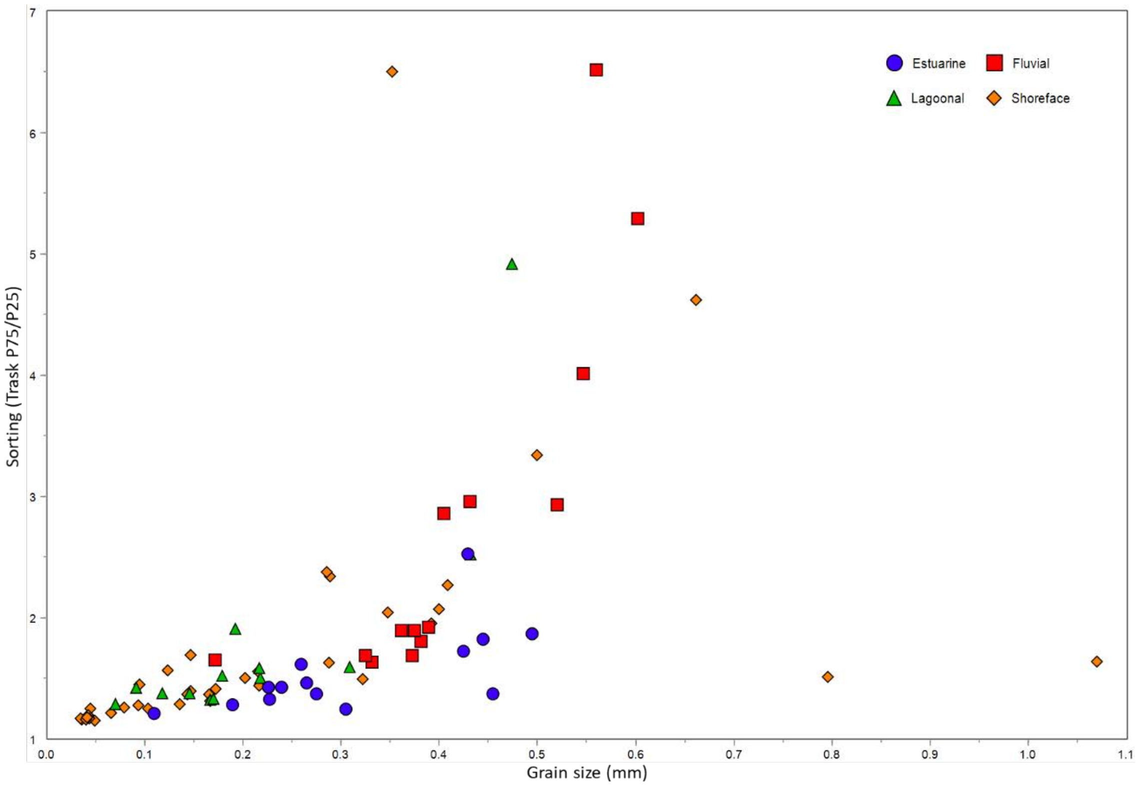

Figure 4.2: *Grain size versus sorting. The most poorly sorted sediments have large mean grain sizes.*

***Table 4.1:** Petrographic, core analysis and burial history data from the studied sandstones given as average values for the Gassum Formation for each well.*

Wells	*Farsø-1*	*Fjerritslev-2*	*Flyvbjerg-1*	*Gassum-1*	*Stenlille-15*	*Stenlille-18*	*Stenlille-19*	*Thisted-3*	*Vedsted-1*	*Aars-1*
Number of samples	*12*	*2*	*4*	*10*	*2*	*7*	*2*	*12*	*6*	*21*
Depth (m)	*2885*	*2304*	*1361*	*1597*	*1563*	*1669*	*1647*	*1204*	*1931*	*3300*
BURIAL HISTORY										
Max burial depth (m)	*3445*	*2989*	*2058*	*2192*	*1971*	*2077*	*2055*	*1896*	*2632*	*3772*
Max temperature (°C)	*112.83*	*98.95*	*71.32*	*77.69*	*69.82*	*72.11*	*71.63*	*68.35*	*88.03*	*123.01*
Max effective stress (Mpa)	*41.65*	*38.27*	*25.45*	*26.71*	*23.46*	*24.19*	*24.03*	*21.52*	*32.38*	*47.29*
Max overpressure (Mpa)	*5.30*	*4.38*	*1.43*	*4.72*	*0.89*	*0.89*	*0.89*	*1.11*	*3.31*	*7.25*
CORE ANALYSIS										
Porosity (%)	*12.30*	*13.32*	*30.91*	*25.42*	*26.19*	*27.91*	*29.39*	*30.44*	*27.79*	*9.91*
Permeability, air (mD)	*116.15*	*16.23*	*4041.48*	*1370.82*	*486.30*	*521.82*	*2446.00*	*2634.37*	*1988.31*	*15.59*
Grain density (g/cm³)	*2.679*	*2.675*	*2.673*	*2.664*	*2.655*	*2.640*	*2.655*	*2.655*	*2.675*	*2.686*
TEXTURE										
Grain size (mm)	*0.266*	*0.119*	*0.193*	*0.162*	*0.290*	*0.362*	*0.208*	*0.275*	*0.223*	*0.363*
Sorting (Trask P75/P25)	*2.085*	*1.432*	*1.529*	*1.489*	*1.554*	*1.655*	*1.222*	*1.875*	*1.592*	*2.455*
Inter-granular volume (%)	*22.76*	*15.01*	*28.23*	*30.79*	*30.26*	*30.11*	*35.32*	*28.45*	*25.88*	*26.82*
Inter-granular porosity (%)	*3.59*	*1.98*	*17.72*	*13.37*	*27.03*	*22.22*	*29.44*	*20.14*	*6.48*	*1.58*
Secondary porosity (%)	*1.39*	*1.25*	*0.64*	*0.99*	*1.42*	*0.35*	*1.19*	*0.33*	*1.87*	*1.70*
DETRITAL PHASES										
Quartz, monocrystalline	*43.69*	*57.04*	*46.45*	*36.36*	*60.75*	*54.49*	*59.09*	*44.69*	*46.17*	*41.66*
Quartz, polycrystalline	*4.56*	*4.53*	*6.70*	*5.82*	*1.95*	*9.20*	*0.96*	*4.42*	*7.90*	*7.09*
K-feldspar	*6.24*	*8.20*	*8.64*	*8.93*	*2.38*	*2.57*	*1.76*	*7.86*	*6.76*	*3.08*
Plagioclase	*14.40*	*7.71*	*2.81*	*8.65*	*0.50*	*0.49*	*0.77*	*8.26*	*4.78*	*12.58*
Mica minerals	*2.16*	*4.14*	*2.03*	*3.24*	*0.14*	*0.03*	*0.21*	*0.63*	*2.49*	*3.16*
Rock fragments	*2.18*	*1.65*	*3.07*	*3.65*	*0.30*	*1.23*	*0.00*	*1.14*	*3.16*	*1.64*
Heavy minerals	*1.25*	*0.30*	*1.02*	*0.69*	*0.43*	*0.34*	*0.14*	*0.92*	*0.88*	*0.89*
Clay matrix	*0.98*	*0.00*	*0.00*	*0.12*	*1.39*	*5.61*	*0.41*	*4.69*	*6.21*	*2.50*
Other detrital	*1.37*	*0.20*	*0.42*	*2.13*	*1.83*	*1.35*	*0.57*	*3.31*	*0.12*	*1.69*
AUTHIGENIC PHASES										
Quartz	*3.91*	*2.94*	*0.12*	*1.08*	*1.70*	*0.45*	*3.85*	*0.08*	*0.97*	*6.82*
Siderite	*0.06*	*5.35*	*9.32*	*4.91*	*0.00*	*0.04*	*0.00*	*1.62*	*3.28*	*0.01*
Calcite	*0.00*	*0.00*	*0.00*	*4.92*	*0.00*	*0.10*	*0.00*	*0.45*	*0.00*	*0.00*
Ankerite	*11.75*	*0.75*	*0.00*	*2.00*	*0.00*	*0.00*	*0.00*	*0.00*	*2.77*	*6.42*
Illite	*0.42*	*0.68*	*0.83*	*1.38*	*0.00*	*0.12*	*0.00*	*0.20*	*1.25*	*2.92*
Chlorite	*0.00*	*0.00*	*0.00*	*0.00*	*0.00*	*0.11*	*0.00*	*0.00*	*0.63*	*0.00*
Kaolinite	*1.18*	*2.55*	*0.16*	*0.68*	*0.14*	*0.83*	*1.56*	*0.42*	*2.37*	*3.87*
Other authigenic	*0.85*	*0.76*	*0.09*	*1.05*	*0.00*	*0.48*	*0.07*	*0.84*	*1.91*	*2.38*

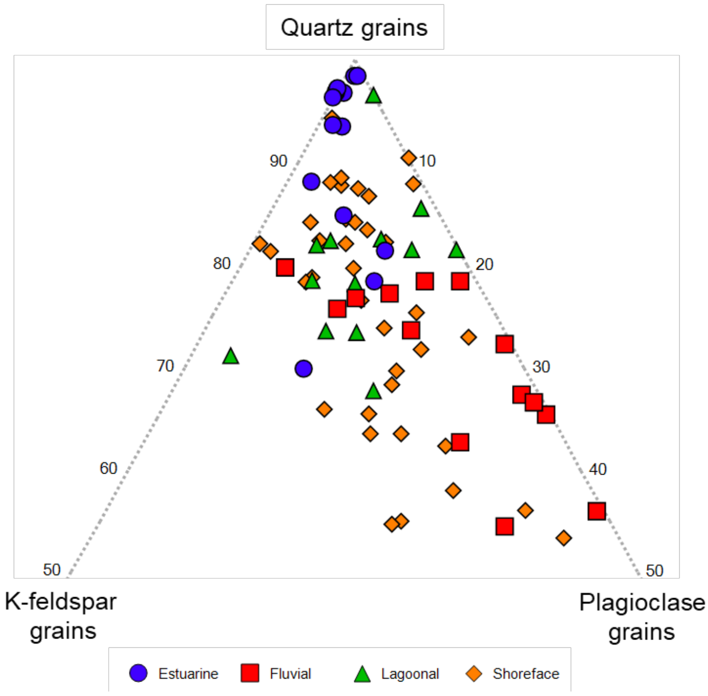

Figure 4.3: *Relative proportions between quartz, K-feldspar and plagioclase grains based on petrographic point counting.*

The authigenic phases comprise 1–44% in the sandstones (average: 14%) (Fig. 4.4). Quartz cement constitutes 0–16% (average: 3%) and clay cement makes up 0–17% (average: 3%) (Fig. 4.5), consisting in decreasing order of abundance of 0–15% kaolinite, 0–12% illite and 0–3% chlorite. Carbonate cements are the most abundant authigenic phase (average: 7%), comprising 0–38% ankerite, 0–31% siderite and 0–37% calcite in decreasing order of abundance (Fig. 4.6). Cements consisting of feldspar, anhydrite, barite, analcime and anatase are present in small amounts (average: <1%, maximum: <3%). Pyrite has formed in most samples in small amounts (average: <1%) and is cementing in a few samples.

Microprobe analysis of the carbonate cements show that the calcite is purely Ca-containing, whereas the siderite beside from Fe also has a significant amount of Mg, Ca and Mn in decreasing order of abundance (Fig. 4.7). The analyzed ankerite from the Gassum-1, Vedsted-1 and Aars-1 wells have a similar composition, whereas most ankerite in the Farsø-1 well has a composition that corresponds more to Fe-dolomite. In general, the carbonate cements changes from being patchy to pervasive with depth (Fig. 4.8). The sandstones in the Gassum-1 well represent a transition zone in carbonate cement type where all three types co-exist (Fig. 4.8A). In the Vedsted-1 well, siderite has formed before quartz overgrowths and ankerite formed after the quartz overgrowth (Fig. 4.8B). Those siderite rhombs that have been enclosed in ankerite are better preserved than those in open pores, however, all siderite is partly dissolved. The morphology of the ragged quartz overgrowths indicates that siderite has been present in many pore spaces and partly prevented quartz overgrowth. The Fe-dolomite/ankerite cement in the Farsø-1 well has a compositional variation with larger Fe-content towards the edged of the cement, and ankerite rhombs have formed in some pore spaces (Fig. 4.8C). The ankerite cement in the Aars-1 well have a deviant composition in a few places, indicating that part of a siderite precursor has been preserved (Fig. 4.8D).

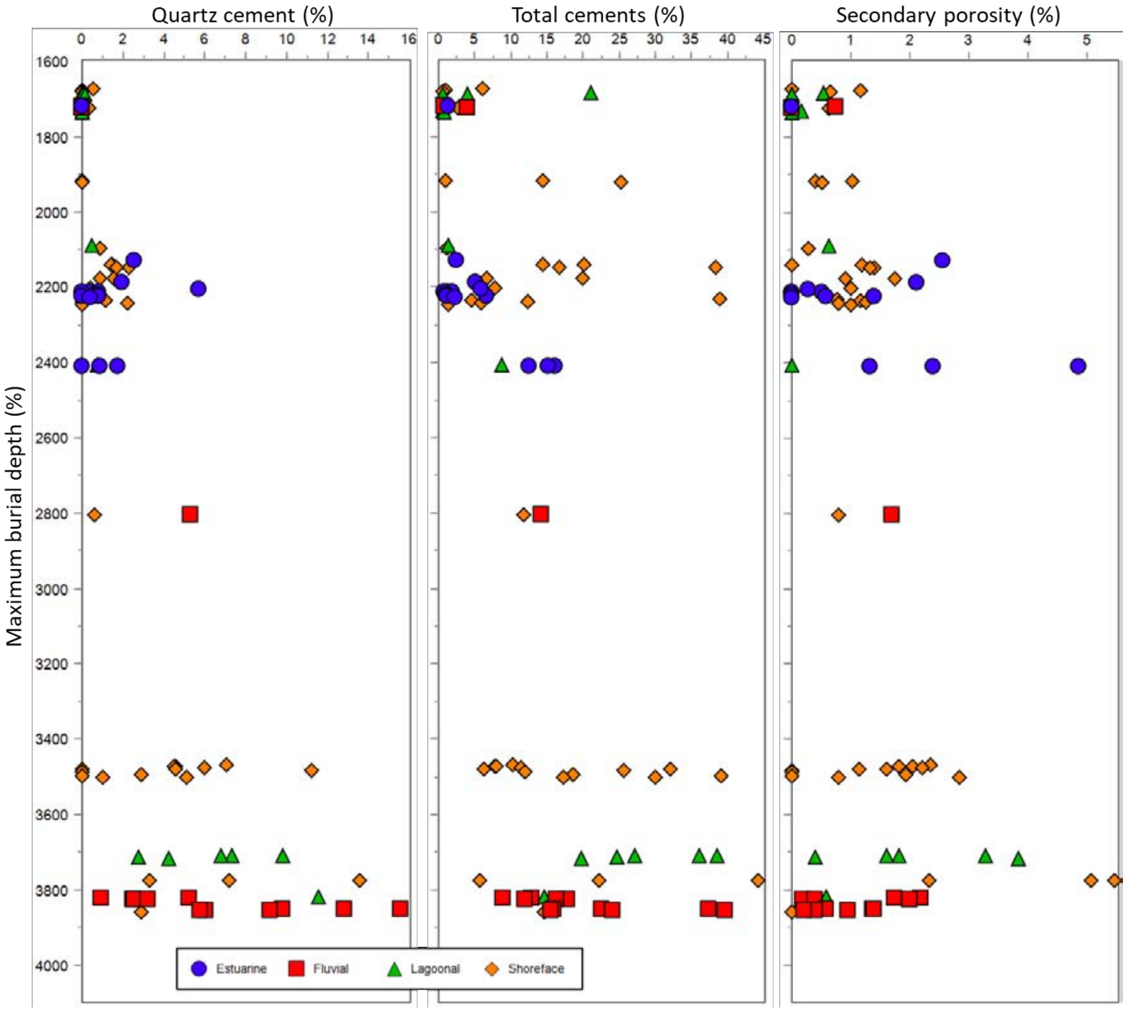

Figure 4.4: *Depth trends in quartz and total cements and secondary porosity.*

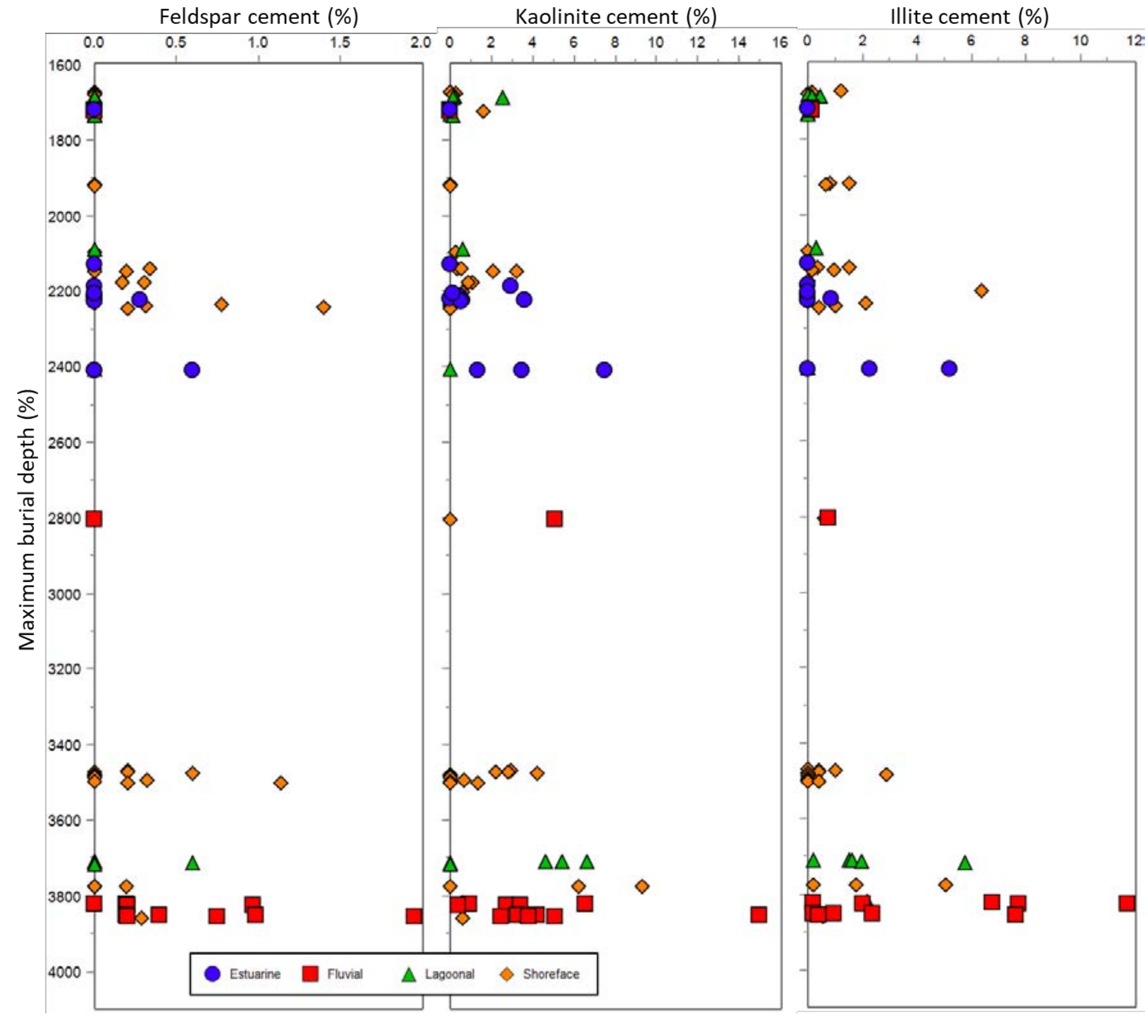

Figure 4.5: *Depth trends in feldspar and clay cement types.*

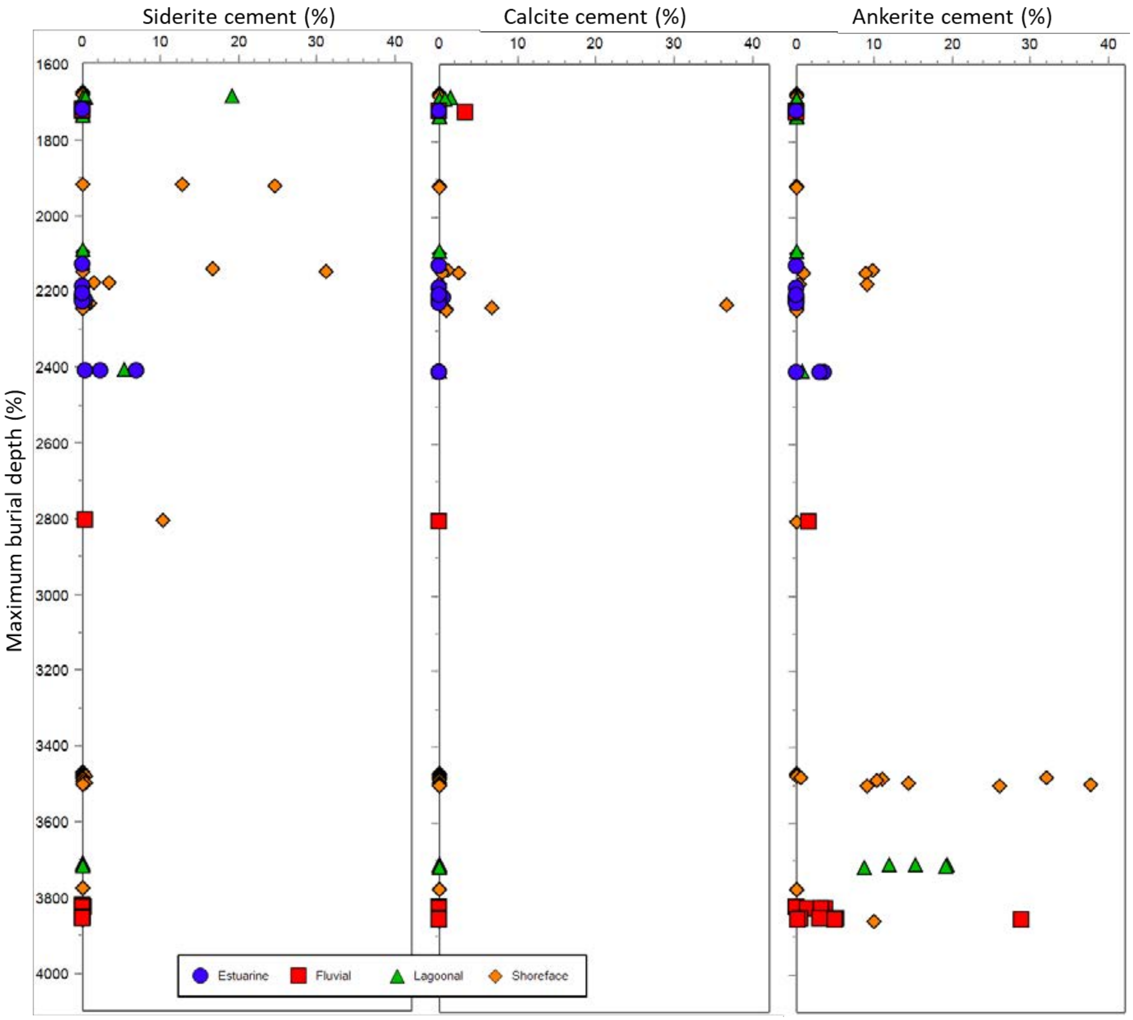

Figure 4.6: *Depth trends in carbonate cement types.*

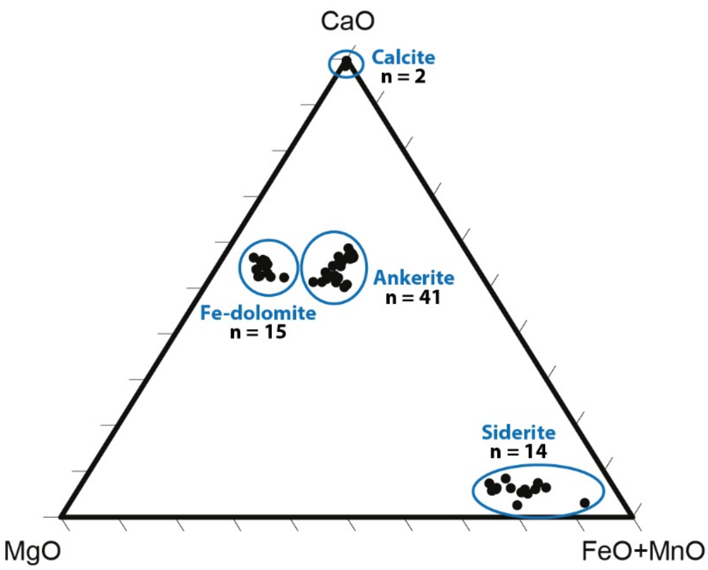

Figure 4.7: *Composition of the carbonate cements in selected samples from the Gassum Formation measured by microprobe.*

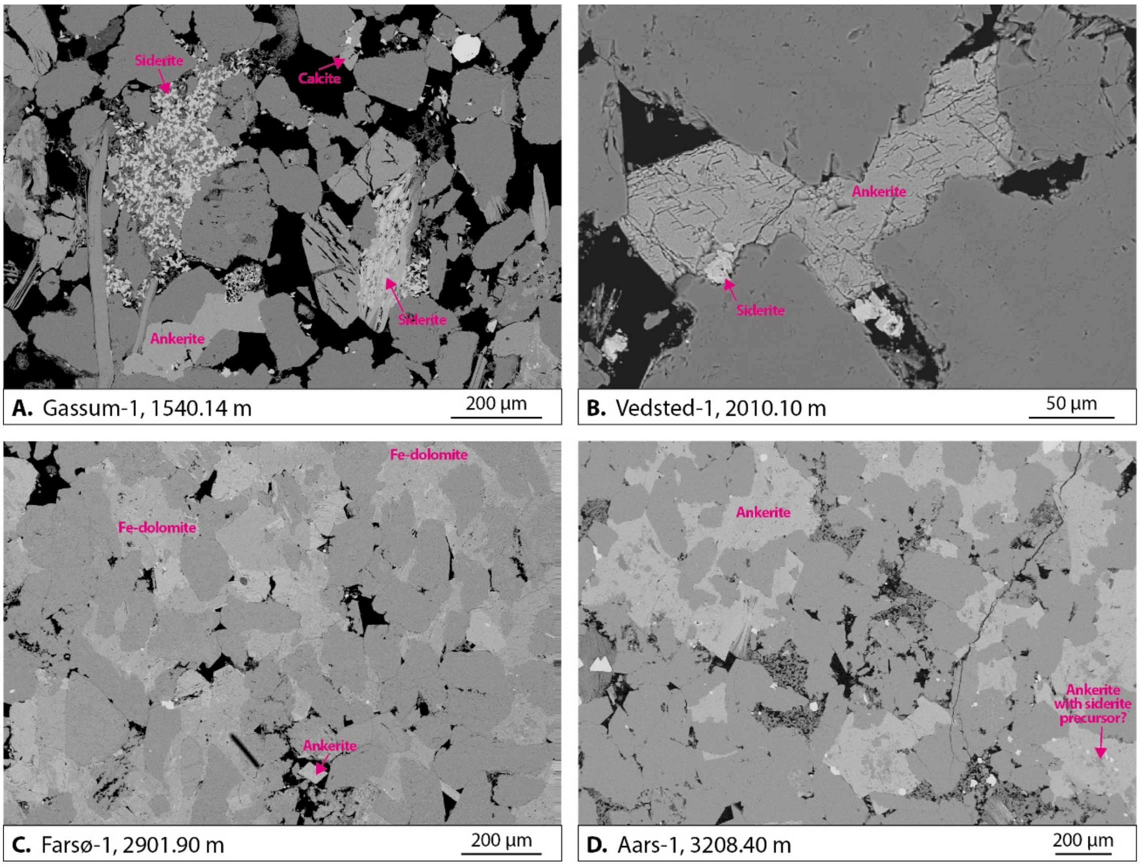

Figure 4.8: *SEM images of the different types of carbonate cement occurring in the Gassum Formation.*

Most samples have poorly coated grains, whereas moderately to well coated grains are more abundant in the deepest part of the formation. The detrital coatings consist of kaolinite and illite, whereas the authigenic coats are primarily consisting of illite besides mixed-layer clays in places. Thin continuous Fe-rich chlorite coatings have only formed during forced regressive conditions and they are found in estuarine and shoreface sandstones (Weibel et al. 2017a).

The measured porosities and gas permeabilities of the studied sediments are 4–35% and 0.05 mD – 12 D, respectively (average: 20% and 1 D) (Fig. 4.9), which cover most of the variation in reservoir properties found in the formation (Fig. 4.10) (Kristensen et al. 2016, Weibel et al. 2017a). In general, the permeability decreases with decreasing grain size. The primary cement type present in each of the studies samples are indicated in Figure 4.9 to show the effect they have on porosity and permeability. Chlorite coatings have a porosity-preserving effect and small amounts of carbonate cement and detrital clays may not decrease the reservoir properties significantly, whereas quartz cement and larger quantities of carbonate and clay decreases the reservoir quality. The secondary porosity quantified by petrographic point counting amounts to 0–5% (average: 1%) (Fig. 4.4), which has mostly formed in dissolving feldspars. The calculated inter-granular volumes (IGV) are 7–45% (average: 27%). The measured grain densities are within 2.61–2.87 g/cm^3.

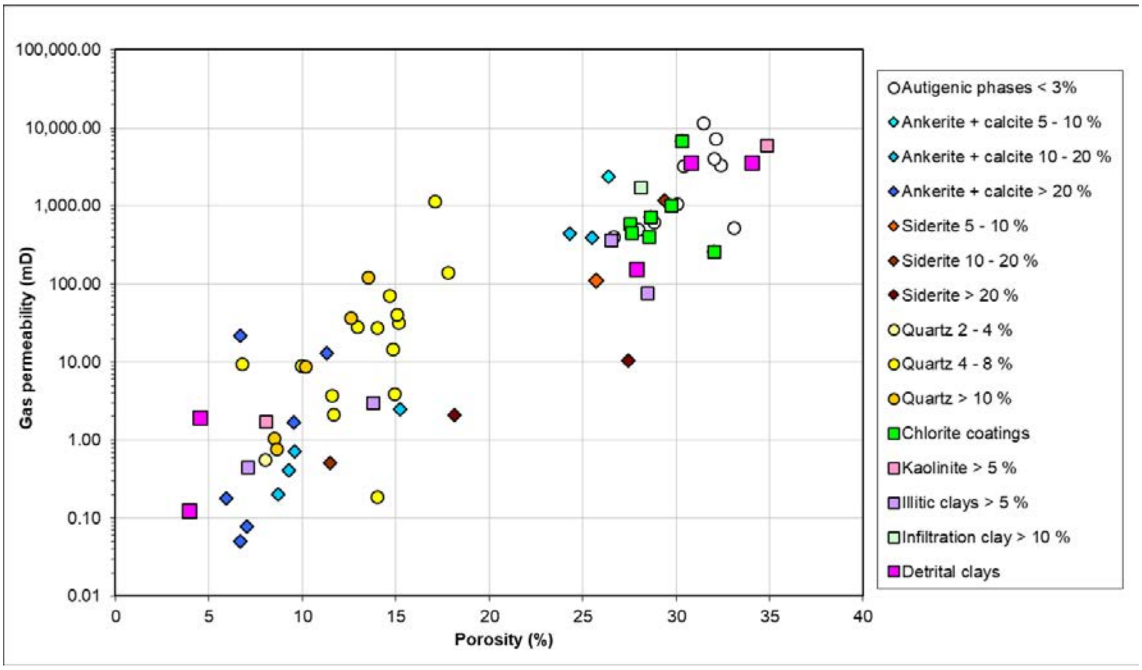

Figure 4.9: *Porosity and permeability for the studied samples with indication of the primary cement types that affect the reservoir properties of each sample. Based on Weibel et al. (2017a).*

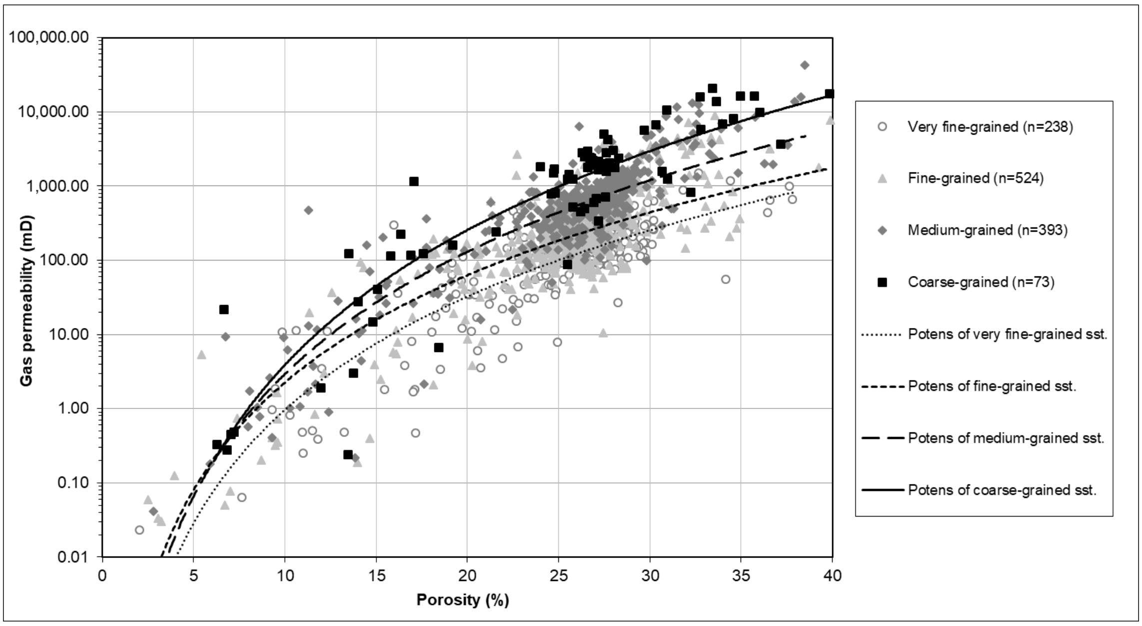

Figure 4.10: *All available porosity-permeability data from the Gassum Formation divided into grain-size classes of very fine, fine, medium and coarse-grained sandstones with trendlines for each class. Based on Weibel et al. (2017a).*

The stressed porosities and fluid permeabilities measured on four samples show that the porosity decreases slightly at increasing pressure from 10 to 300 bar, whereas the permeability decreases considerably (Fig. 4.11). The comparison between gas and fluid permeabilities show that the relationship is not uniform, but the fluid permeabilities are significantly lower that the gas permeabilities. The compressibility measured by the produced water during the experiments shows that most compression occurred at low pressures for the three samples from the Farsø-1 and Aars-1 wells where the Gassum Formation has been deepest buried. Hence, even though the maximum stress of 300 bar during the experiments is not as high as the maximum effective stress of c. 416–471 bar they have been exposed to during burial, measurements at higher stress would presumably not have reduced the reservoir properties significantly. The two shallower samples from the Gassum-1 well have experienced effective stresses of up to c. 261–268 bar during burial and especially one of the samples shows high compressibility at 200–300 bar.

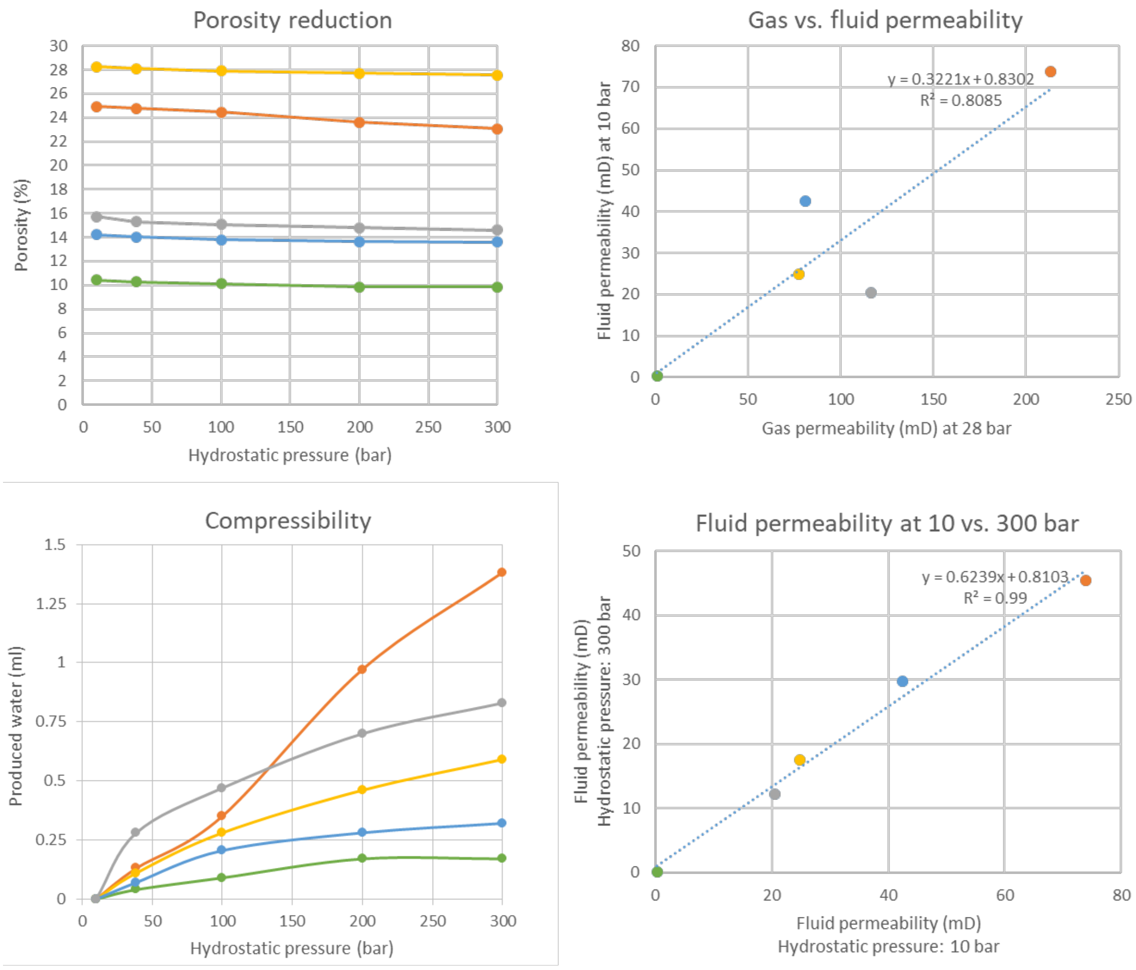

Analyzed samples:

Well	Present-day depth (m)	Max burial depth (m)	Max effective stress (bar)
Gassum-1	1539	2134	261
Gassum-1	1603	2198	268
Farsø-1	2873	3433	416
Farsø-1	2902	3462	418
Aars-1	3275	3747	471

Figure 4.11: *Porosity and permeability of five of the studied sandstones from the Gassum Formation measured at increasing pressure. The volume of produced water has been recorded to estimate the compressibility of the sandstones. The fluid permeability results are compared to results of standard gas permeability measurements.*

4.2 Mineralogical temperature constraints

The homogenization temperatures of fluid inclusions in quartz cement were measured for three samples and they are in the interval of 107–129°C (Fig. 4.12). The fluid inclusions are very small in the Gassum Formation, so it was only possible to analyze samples from the deepest part found in the Farsø-1 and Aars-1 wells. Only inclusions that were with certainty present in the overgrowths were analyzed, which may explain why the lower temperatures at which the cement began precipitating are not recorded in the analyses.

The oxygen isotopic composition in ankerite and dolomite cement in the Aars-1 core suggests minimum burial temperatures of 120°C (Table 4.2), based on the temperature-related formula for $\delta^{18}O$ composition in carbonates by Zheng (1999). This is supported by the common albitization of feldspar, which typically takes place at temperatures of 100–130°C (e.g. Aagaard et al. 1990, Mansurbeg et al. 2008). The burial temperatures are minimum 110°C according to ankerite and dolomite cement in the Farsø-1 core. This is also supported by common albitization. Minimum burial temperatures of 100–105°C in the Vedsted-1 core is achieved from the oxygen isotopic composition of ankerite and dolomite cement. Incipient dickite precipitation between booklets of kaolinite (Weibel et al. 2017a) supports this as a minimum temperature (compare with Beaufort et al. 1998).

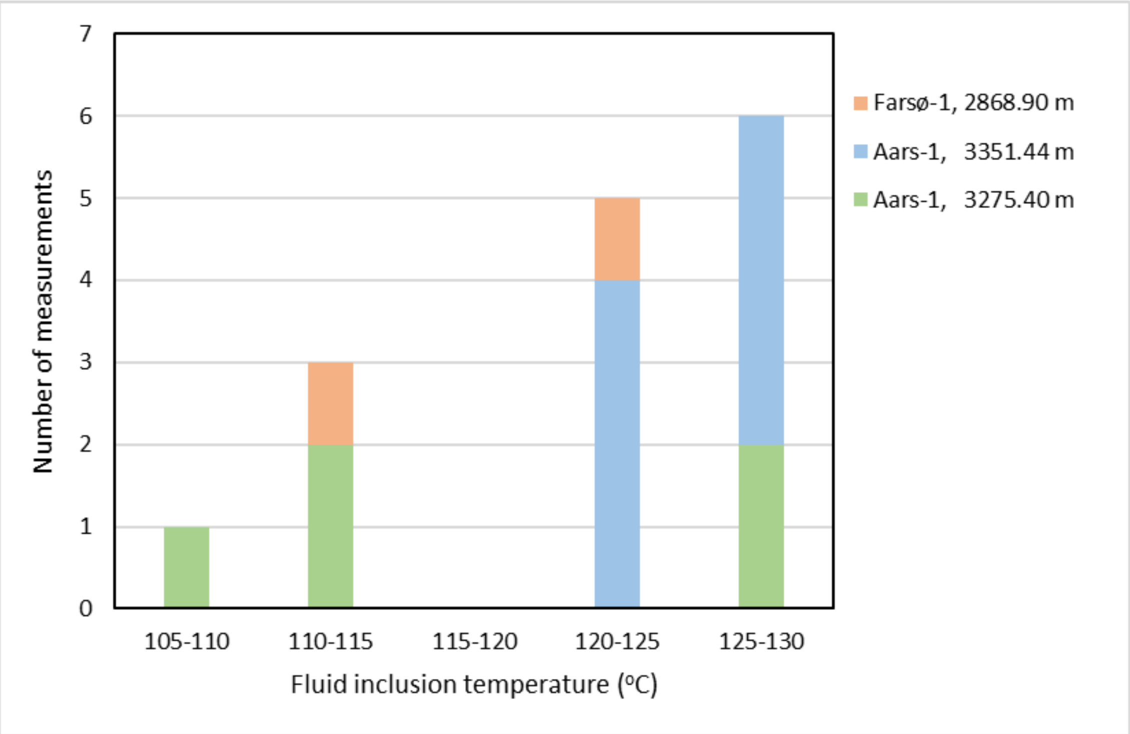

Figure 4.12: *Fluid inclusion data measured as the homogenization temperatures of fluid inclusions in quartz cement. The present-day burial depths of the samples are shown.*

Table 4.2: *Temperature indicators achieved from petrographic investigations of the Gassum Formation. The temperature estimates are based on average $\delta^{18}O$ values for calcite by application of the formula by Horibe and Oba (1972) or Zheng (1999), and for ankerite and dolomite by Zheng (1999).*

		Diagenetic suggested maximum burial				
		Mineralogical constraint	Temp. indication (either from comparison with literature or from calculation of $\delta^{18}O$)	Temp. calculated	Difference between recent and maximum burial depth (m)	
Well	**Depth (m)**				**Mineralogical**	**$^{Neo}dZ_B$***
Aars-1	3350	Albitization	65-120°C (Aagaard et al. 1990), 100-130°C (Mansurbeg et al. 2008)	115.5	500	500
	3360	Ankerite isotopic composition	122-125°C	121.8	700	
	3210	Dolomite isotopic composition	119-123°C	120.3	800	
Farsø-1	2880	Ankerite isotopic composition	108-115°C	110.4	800	600
	2880	Dolomite isotopic composition	113-117°C	113.4	900	
	2880	Albitization	65-120°C (Aagaard et al. 1990), 100-130°C (Mansurbeg et al. 2008)	101.4	500	
Gassum-1	1600	Common quartz overgrowths	> 80°C (Bjørlykke et al 2010 etc.)	72	800	600
Vedsted-1	2010	Dickite precipitation	3300 m (Beaufort et al 1998)		1290	
	1775	Ankerite isotopic composition	111-114°C	98.3	1500	
	2010	Dolomite isotopic composition	108°C	105.3	1500	

4.3 Basin modelling with PetroMod

Based on the tectonic-stratigraphic framework defined in the Danish onshore area, the selected wells are divided into layers or events allowing the 1D PetroMod software to quantify all important basin processes as a function of time, including maturity parameters such as temperature and vitrinite reflectance. The 1D PetroMod model is calibrated against maturity data using either the EASY%Ro (Sweeney and Burnham 1990) or the Basin%Ro (Nielsen et al. 2015) vitrinite reflectance models to determine the thermal evolution of the basin. The boundary conditions are paleo-water-depth (PWD), sediment water interface temperature (SWIT) and basal heat flow (HF). The boundary conditions define the basic energetic conditions for the temperature development for all layers through time. The SWIT for each model event is derived using a build-in method in PetroMod© that based on a world-wide database and the hemisphere and continental location of the Danish area through time, assigns sediment water interface temperatures. Estimates of paleo-temperature were derived from these paleo-climatic models included in the software (Wygrala 1989) for 54°N. Thus, the calculated temperature history is based upon standard mathematical approximations of heat flux in sedimentary basins through time, which is expressed as the HF model, together with SWIT through time, composition and thickness of the sedimentary infill, potential erosion and timing (Japsen and Bidstrup 1999, Nielsen 2003, Japsen et al. 2007).

At each 1D model well location, the paleo-heat flow history is calibrated against the vitrinite reflectance and temperature data. In order to keep the temperature history simple and to insure direct comparison between the temperature history used in SURP, the following assumptions and simplifications were made:

- Due to uncertain information on the Middle Cimmerian Unconformity (MCU), it is assumed that the amount of missing Fjerritslev Formation (i.e. F-III and F-IV) is <350 m. This estimate may be too low since erosion of the formation occurred in most places and the formation thickness is >1000 m in some of the places where it has not been eroded, so the burial histories by Nielsen (2003) may be more realistic with their larger estimates of Middle Jurassic uplift and erosion. However, the difference would not have had much influence on the diagenesis modelling since the Gassum Formation was shallowly buried at the time.
- PWD is a constant of 0 m throughout the modelling history.
- To insure maximum temperature at maximum burial, a constant of SWIT of 5°C should be assumed throughout the modelling history. However, to follow the standard modelling concept used throughout the Danish area, SWIT is taken from the build-in method by Wygrala (1989). In order to match the calibration data, a simple uniform heat flow history has been applied insuring that the maximum temperature of c. 125°C at the Aars-1 location match the information from fluid inclusion and carbonate cement isotope data.

To show the variation in the burial and temperature history in different parts of the Danish onshore area, Aars-1 and Stenlille-1/area were selected as representative examples (Fig. 4.13). The match with calibration data at these two locations are presented in Figure 4.14. The results show that optimisation of vitrinite reflectance with the Basin%Ro model seems to give the best match. To get the optimal match with the temperature data, a slightly higher thermal gradient of c. 28–30°C/km is necessary. The burial histories for all the wells used in this study are included in Figure 4.15.

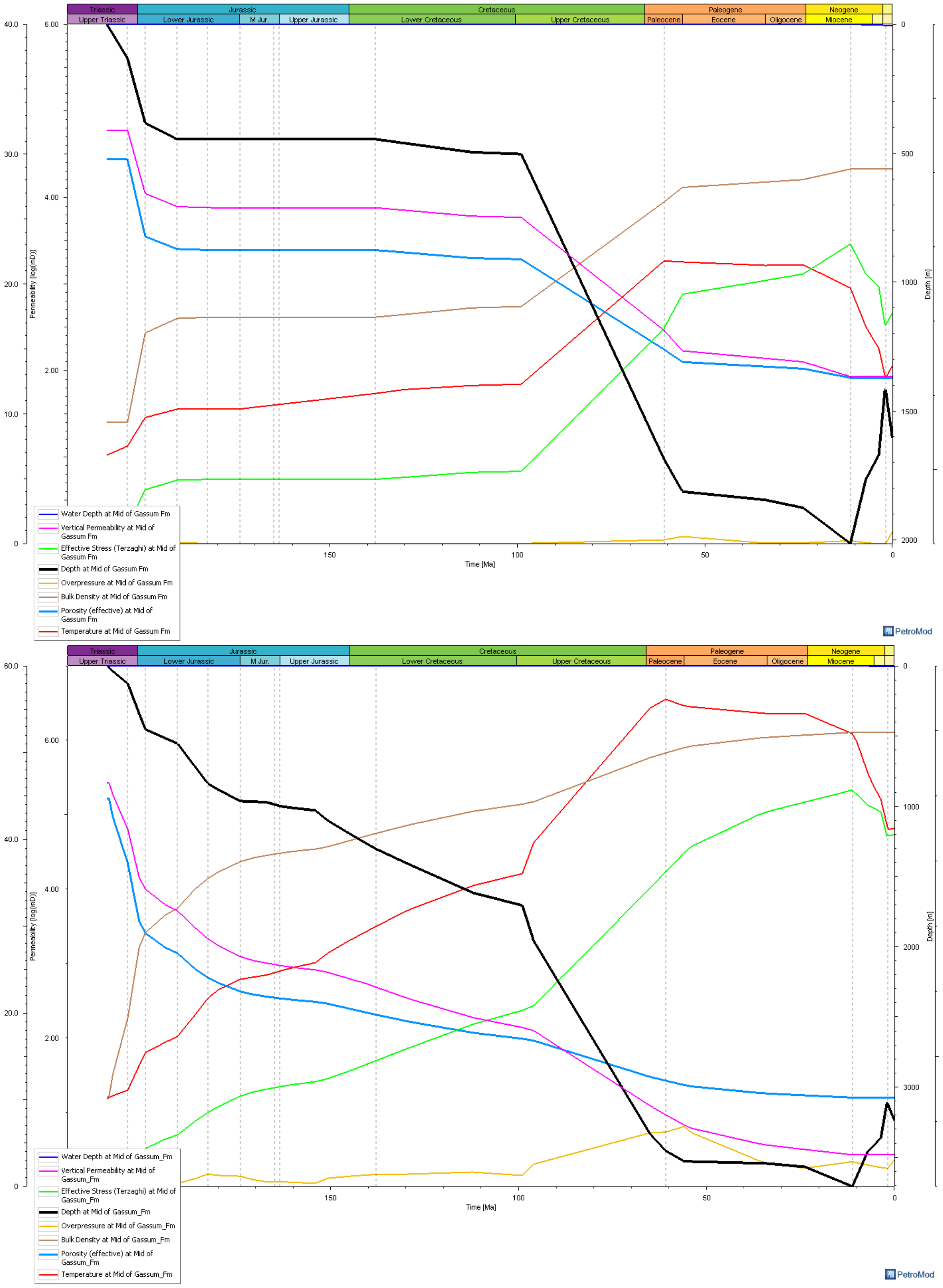

Figure 4.13: *PetroMod modelled burial history (in black) and temperature development for the middle of the Gassum formation for the Stenlille area (upper) and the Aars-1 well (lower).*

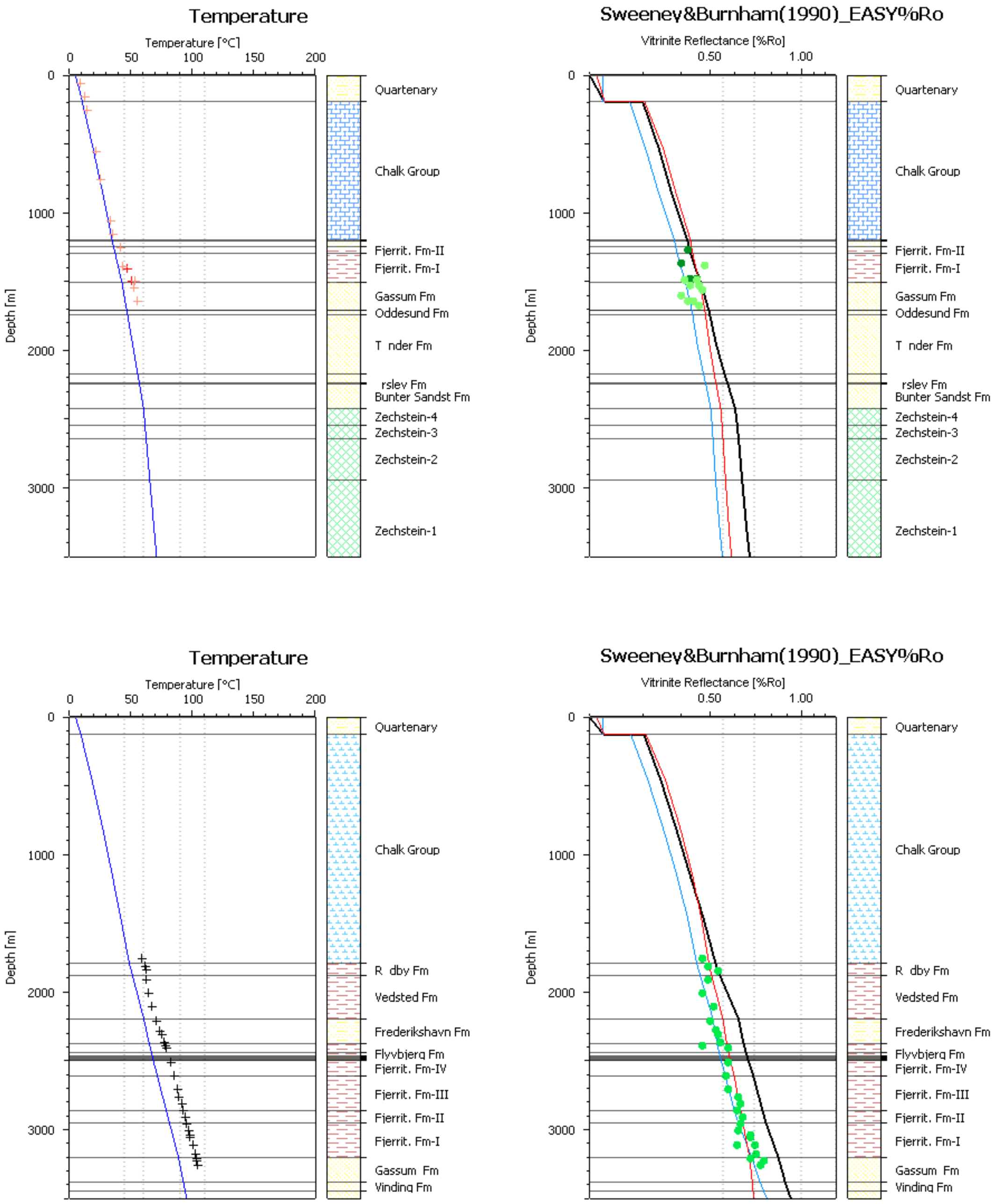

Figure 4.14: *Calibration at the Stenlille area (upper) and at the Aars-1 well location (lower) with temperature (left) and vitrinite reflectance (right).*

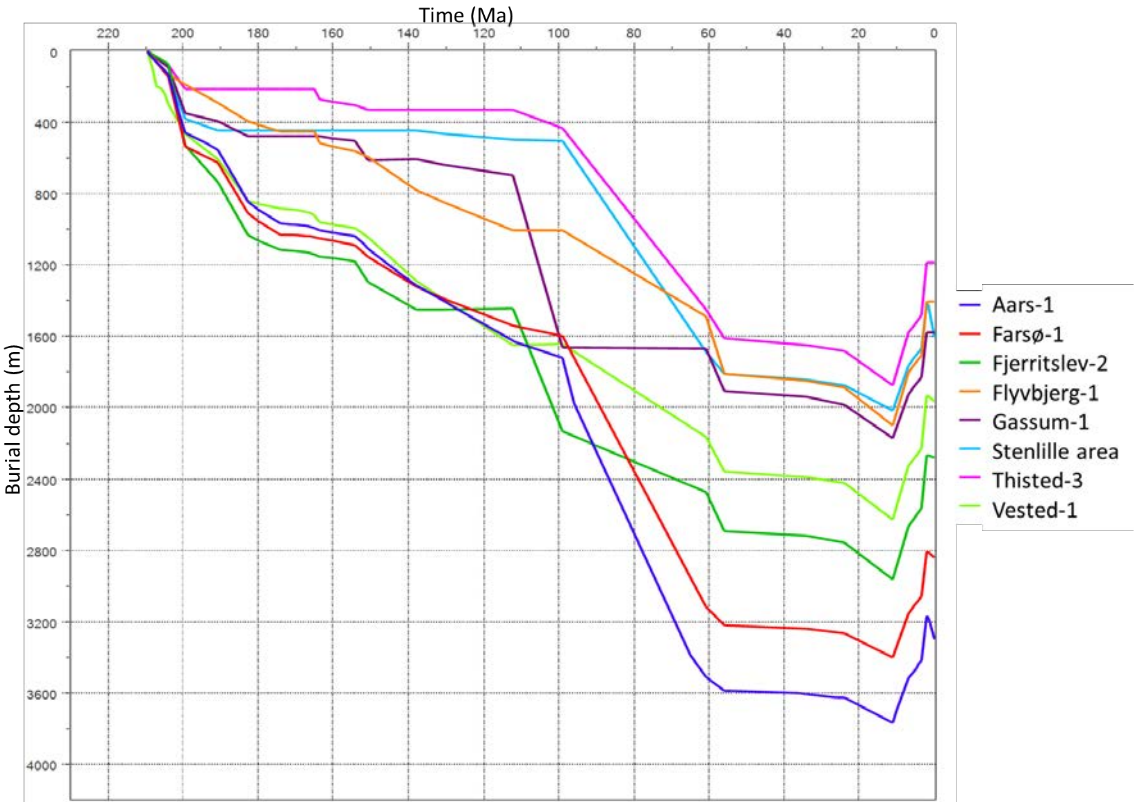

Figure 4.15: *Burial histories derived from basin modelling and employed in the Touchstone modelling.*

4.4 Diagenesis modelling with SURP

Burial of the Gassum Formation is recalculated using SURP and the result is comparable with the burial histories calculated using PetroMod (Fig. 4.16). Some differences in burial depth and formation thickness exist between the burial histories modelled by PetroMod and SURP because of compaction parameters that can differ in the two burial simulations. Simulations with SURP were stopped at the maximal burial depth before the late Cenozoic exhumation.

Temperature evolution during burial is directly dependent on depth in SURP calculations since temperature was calculated using one geothermal gradient constant over time. In the PetroMod model, geothermal gradient or thermal flux was changed over time according to various indicators of temperature evolution. Therefore, some differences are seen between the temperature evolution calculated with the two modelling approaches (Fig. 4.17). Since diagenetic reactions are strongly linked to temperature, the temperature calculations with SURP focused on reaching the same maximal burial temperature as the one reached using PetroMod. This maximum temperature is reached at the end of the simulation with SURP while it is reached earlier with PetroMod since the geothermal flux was decreasing during the Cenozoic, even before the late exhumation.

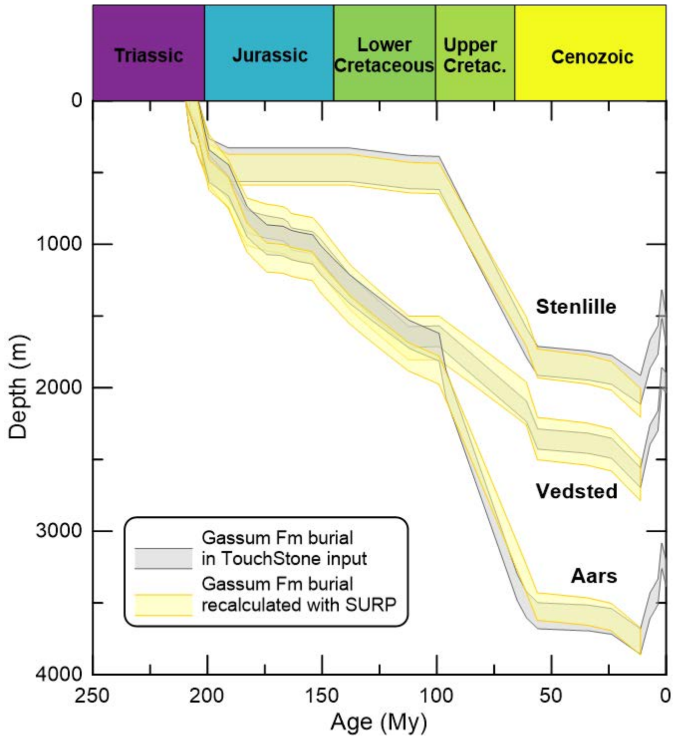

Figure 4.16: *Burial and thickness evolution of the Gassum Formation calculated using PetroMod to the Touchstone modelling and recalculated with SURP for the Aars-1, Vedsted-1 and Stenlille wells. The depth corresponds to the maximum burial depth and uplift is only modelled by PetroMod.*

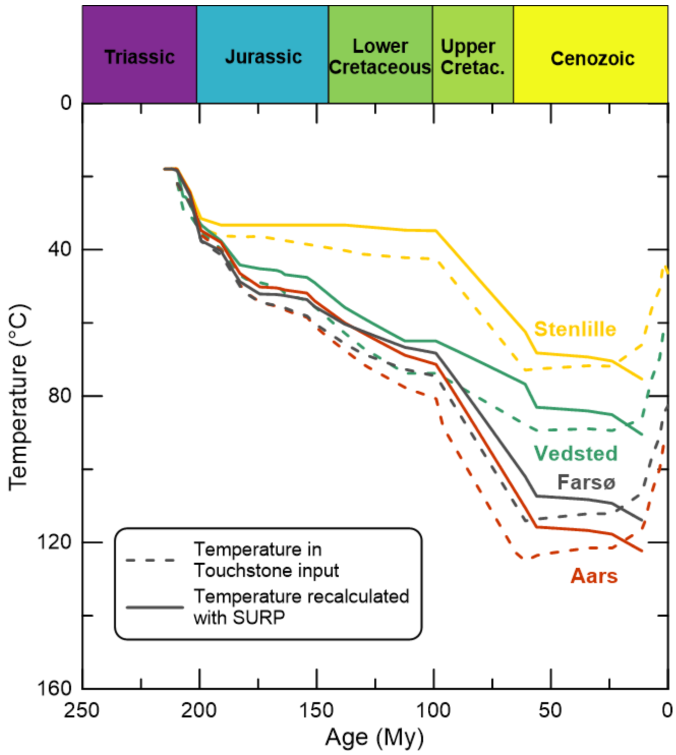

Figure 4.17: *Temperature evolution at the base of the Gassum Formation calculated using PetroMod to the Touchstone modelling and recalculated with SURP.*

Diagenetic modelling with SURP of Gassum Formation sandstones during burial shows quartz cement as the main mineral precipitate and the quartz precipitation started between 1500 and 2000 m (Fig. 4.18). The formation of quartz cement increased with depth to c. 7% at the deepest burial. These simulation results are in line with the observed amounts of quartz cement in the studied samples, despite the natural scattering of the data. Other silicates that were predicted to precipitate include kaolinite and illite, both in abundances of c. 1%. No chlorite was calculated to form. Kaolinite formed deeper than expected in the simulations and adjustment of model parameters was not able to fit with a shallower precipitation of kaolinite, as observed in samples. In agreement with the petrographic observations, illite was calculated as the latest aluminosilicate phase to precipitate.

Calcite and siderite were modelled as initial carbonate cements and were simulated to dissolve and be replaced by ankerite, which formed in amounts of about 2% at the deepest burial. Several steps of ankerite formation were simulated with depth, in link with the formation of illite, suggesting a competition with respect to the availability of Mg released by the initial carbonate cements.

The porosity evolution with depth calculated with SURP is reported in Figure 4.19, where one model scenario comprises only the effect of mechanical compaction and the other model scenario shows the combined effect of compaction and mineral volume changes due to diagenesis. In agreement with the calculated diagenetic evolution, the porosity governed by diagenesis was simulated to be different from the one driven by compaction, starting at about 1500 m depth where the porosity is calculated to be c. 30% when considering an initial porosity of 40%. The difference between the two scenarios become progressively more pronounced with depth where a porosity of c. 25% is calculated by compaction alone in the deepest part of the reservoir whereas a porosity of c. 15% is obtained when considering both compaction and diagenesis. In comparison with the measured gas permeabilities, the calculated porosity is lower than average in the shallow part of the reservoir and higher than average in the deep part of the reservoir.

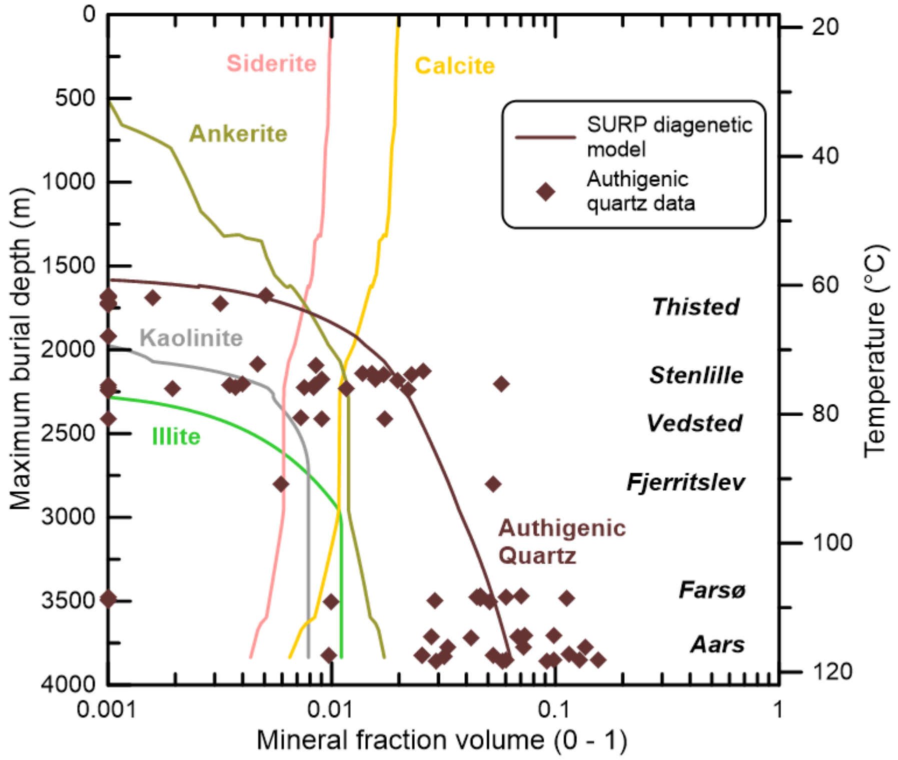

Figure 4.18: *Simulated diagenetic evolution of Gassum Formation sandstones with depth using SURP. The modelled amount of authigenic quartz is compared with the measured values. Well names are shown at the maximum burial depths that the Gassum Formation has experienced in these wells.*

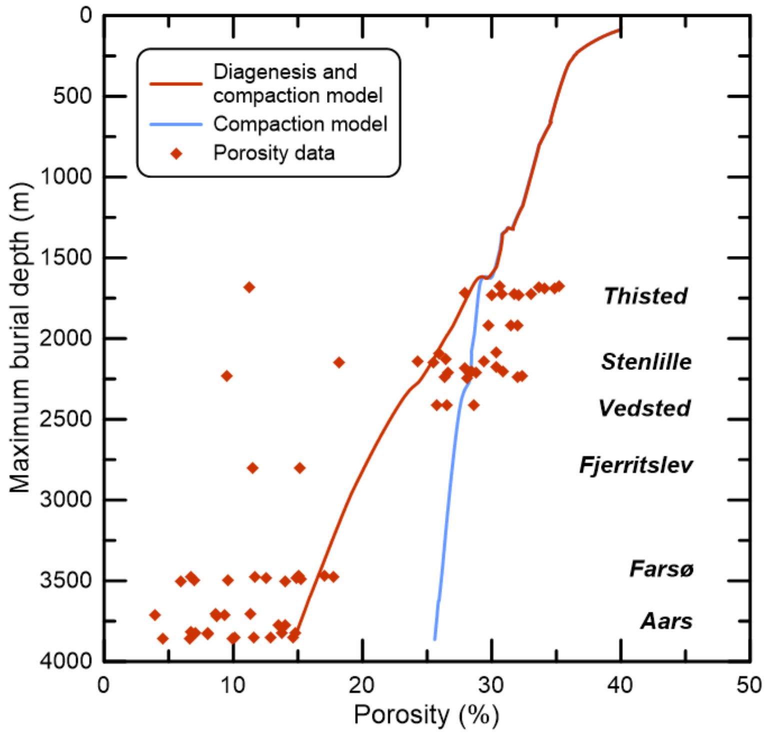

Figure 4.19: *Comparison between measured porosities and calculated porosity evolution in Gassum Formation sandstones using SURP. One model scenario includes only the effect of compaction, whereas the combined influence of compaction and diagenesis is shown in the other scenario.*

4.5 Diagenesis modelling with Touchstone

The results of petrography and reservoir properties of the analyzed samples are employed in the Touchstone diagenesis modelling, except for data from the Farsø-1 well that will be used to validate the model. About a third of the samples were randomly selected as test samples, which are not considered in the modelling. Simulation of the samples was followed by optimization of the model by finding the parameters that best match the measured values. The optimization results show good correlation between the measured and calculated quartz cement volumes and permeabilities (Figs 4.20, 4.21). The test samples display about equally good performance as the calibration data, showing that the modelling is robust (Fig. 4.20). The fluvial sandstones seem to be most complicated to model and are in general also those with the most advanced diagenesis (Fig. 4.21).

Optimization of the model gives a permeability correction factor of about five, meaning that the calculated permeabilities are multiplied by five to match the measured gas permeability values. This conforms with the stressed porosity and permeability measurements, which show that the gas permeabilities must be divided by a factor of about five to correspond to the fluid permeabilities at reservoir pressure (Fig. 4.11).

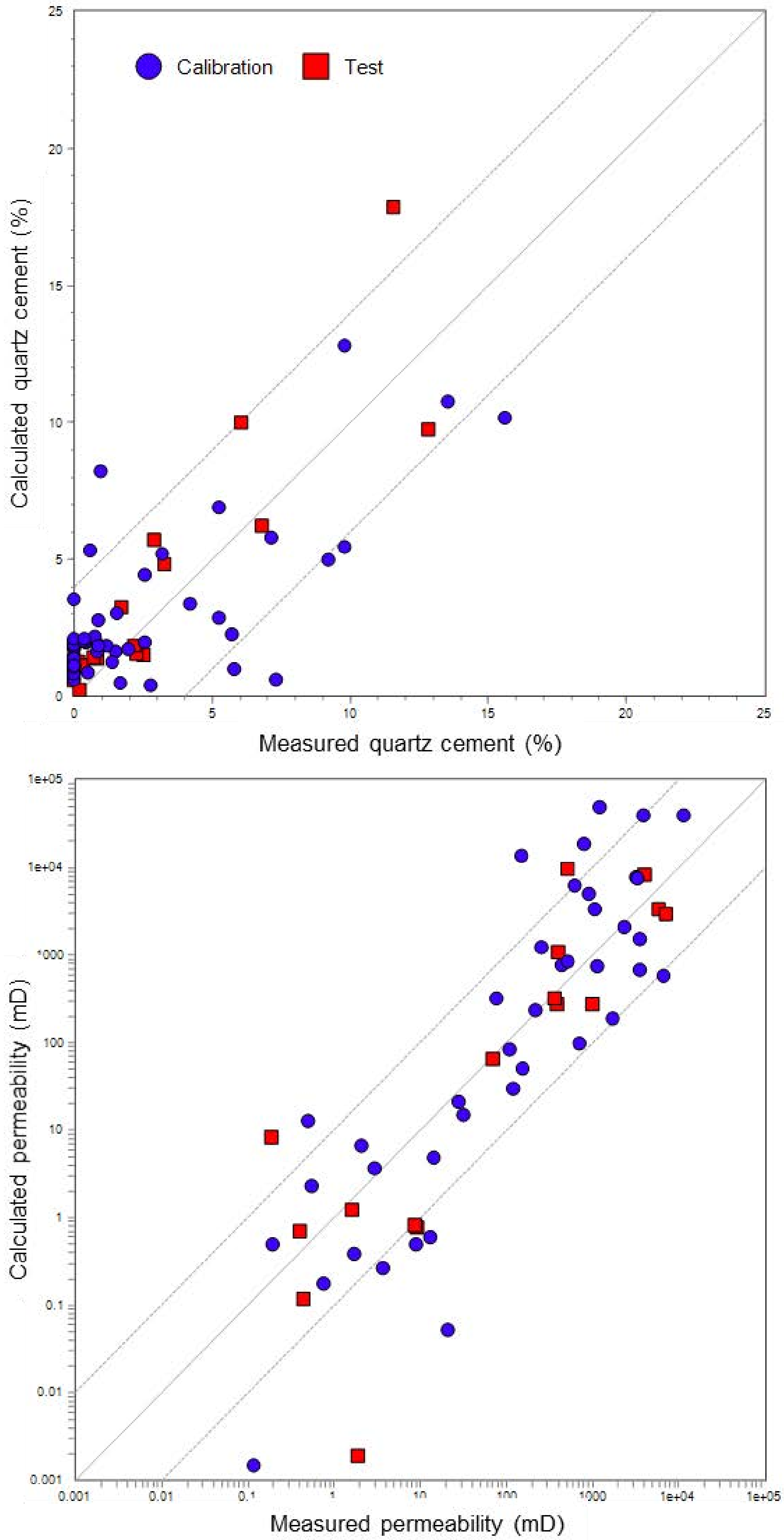

Figure 4.20: *Measured versus calculated quartz cement volume and permeability of the Gassum Formation excluding data from the Farsø-1 well since they are used to validate the model. The sample symbols show which data are used for calibration and for testing, respectively.*

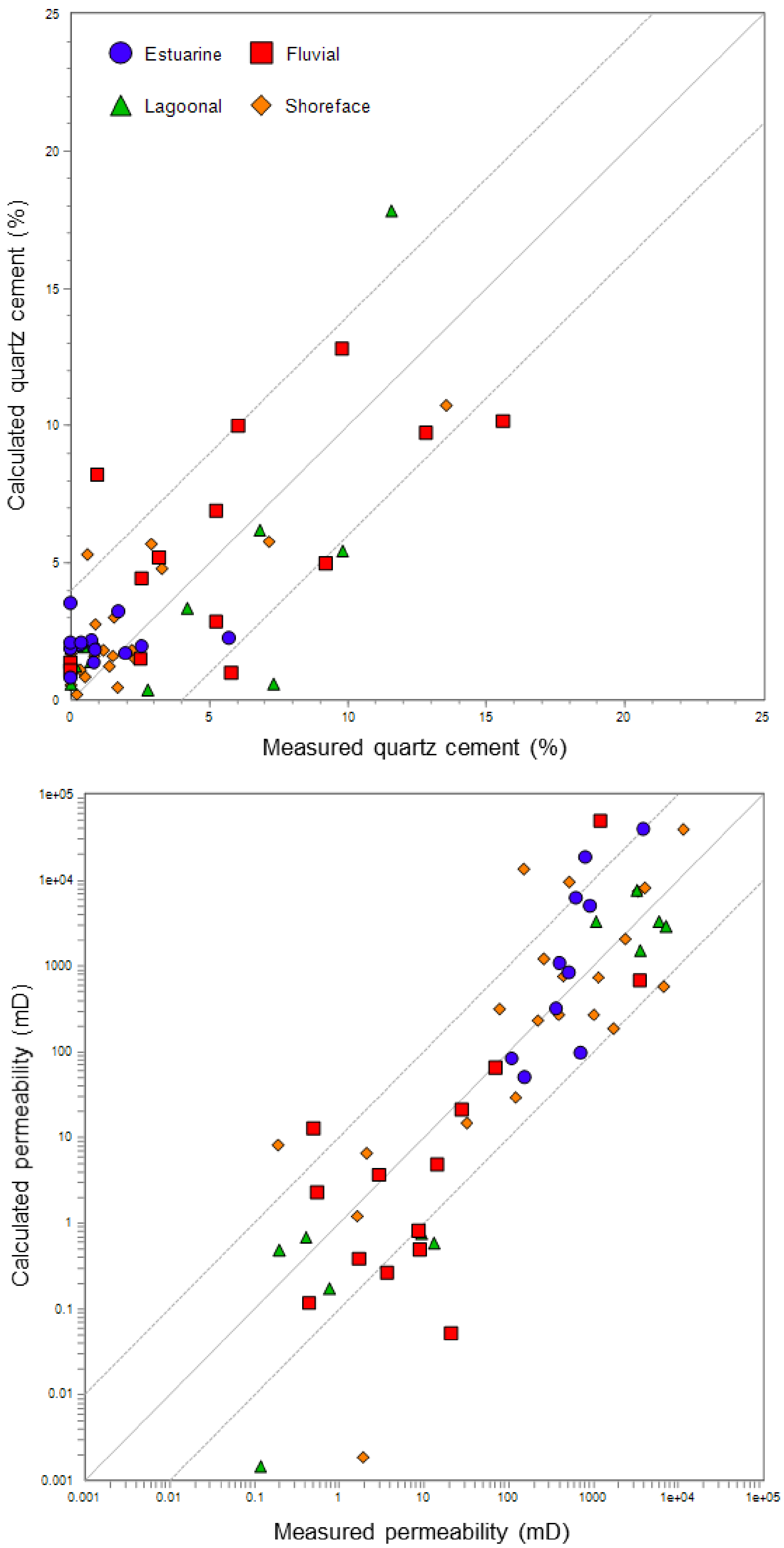

Figure 4.21: *Measured versus calculated quartz cement volume and permeability of the Gassum Formation excluding data from the Farsø-1 well since they are used to validate the model. The sample symbols show which depositional environment they belong to.*

5. Prediction

5.1 Conditions for ankerite precipitation

Carbonate cement is one of the diagenetic alterations that may reduce the reservoir quality significantly. However, the conditions for carbonate mineral precipitation and alteration cannot be modelled at present with Touchstone, although the amount may be simulated in pre-drill estimates by considering the composition of samples buried at about similar depths or by including knowledge from other sources.

Carbonate minerals and the carbonate chemical system can be considered with the SURP code. Additional calculations with the code were made to investigate which chemical conditions are favorable to the formation of large amounts of carbonate minerals as observed in especially shoreface facies sandstones from the Gassum Formation, as well as in some of the other depositional environments (Fig. 4.6).

Among several tested conditions, the availability of Mg in the pore water proved to be essential in providing favorable conditions for ankerite precipitation. Figure 5.1 reports a calculation case where the concentration of Mg was increased by a factor of five in the formation water (0.4 mol/L of Mg instead of 0.08 mol/L) and a second case where the Mg concentration and the amount in initial carbonates were increased. When only the Mg concentration was increased, ankerite started precipitating at shallower depth than during lower Mg concentration (Fig. 4.18) and the amount of ankerite was larger but precipitation stopped when the initial siderite and calcite were entirely dissolved (Fig. 5.1A).

This shows that Mg is the limiting factor in the carbonate system evolution and that increasing the Mg amount in the pore water displaces the equilibrium towards a higher precipitation of ankerite, which destabilizes initial calcite and siderite. This calculation case with a higher Mg content also shows that precipitation of Mg-bearing illite and chlorite is favored rather than quartz and kaolinite, respectively, once the precipitation of ankerite stop.

When the Mg content in the pore water and the amount of initial carbonate minerals were both increased, then ankerite precipitation was no longer limited by the availability of calcite and siderite and up to 6% ankerite was simulated to precipitate (Fig. 5.1B). Illite and chlorite also precipitated in higher amounts than in the base calculation case with no increase of the Mg content in the formation water (compare Fig. 4.18 with Fig. 5.1B), but the Mg was preferentially used for the ankerite precipitation. Quartz precipitation occurred in similar amounts as in the base case. Similar sensitivity analysis to the Fe content in the pore water was made, but the diagenetic sequence results did not change comparatively to the base case, indicating that Fe is in excess in the chemical system.

This sensitivity of the carbonate mineral evolution to the availability of Mg in the pore water indicates that an additional source of Mg is required to explain the high amounts of ankerite observed in some samples (Fig. 4.6). This source of Mg could be Mg-rich detrital minerals, Mg-bearing carbonates or Mg-rich water entrance during burial. The sandstones do not contain much smectite, but the smectite-illite transformation in deeper or interbedded mudstone intervals could possibly have supplied enough Mg for the ankerite formation. This is one possible triggering mechanism for the timing of when the ankerite precipitation begins. Another possible triggering mechanism could be related to the maturing of organic matter where released CO_2 may dissolve the initial carbonate minerals, which may then precipitate as other carbonate mineral types in relation to the evolved pore water composition.

An initial source of carbonate is needed in order for ankerite to form during burial, and this source could be either carbonate clasts, carbonate fossils and/or carbonate cements formed at shallow burial. Sensitivity studies performed in the SURP modelling shows that ankerite precipitation is favored by the presence of both calcite and siderite. In the case with 1.4% calcite and 0.6% siderite that dissolves due to high Mg content in the pore water (Fig. 5.1A), the calcite is consumed first and then the ankerite precipitation declines and stops completely a few hundred meters deeper when the siderite is also consumed. If considering a case with 1% calcite and 2% siderite, then ankerite precipitation decreases significantly when calcite vanishes because Ca is no longer supplied by the calcite dissolution, so some siderite is preserved even at large depths.

These results are in agreement with observations from the Gassum Formation where no calcite is present at maximum burial depths larger than 2300 m, whereas significant amounts of siderite can occur as deep as at least 2800 m and small siderite amounts of <1% are found in even a few of the deepest samples from the Farsø-1 and Aars-1 wells (Fig. 4.6).

When considering a case where only siderite and no initial calcite is present, the precipitation of ankerite is small and slow. When considering a case where only calcite and no initial siderite is present, the reactivity and ankerite precipitation is also smaller, which indicates that a limitation in Fe can be reached under these conditions. A supply of Fe is then also required for ankerite precipitation.

It must be considered that thermodynamic models have inherent limitations since only pure phases can be used in the modelling, so the employed calcite phase contains only Ca and the siderite phase contains only Fe (Table 3.1). In addition, problems exist with the coexistence of various phases presenting neighbouring compositions such as for example dolomite in the present case. Despite these limitations, the thermodynamic modelling gives important insights concerning the reactive sequence and helps identify the favorable conditions for given precipitations.

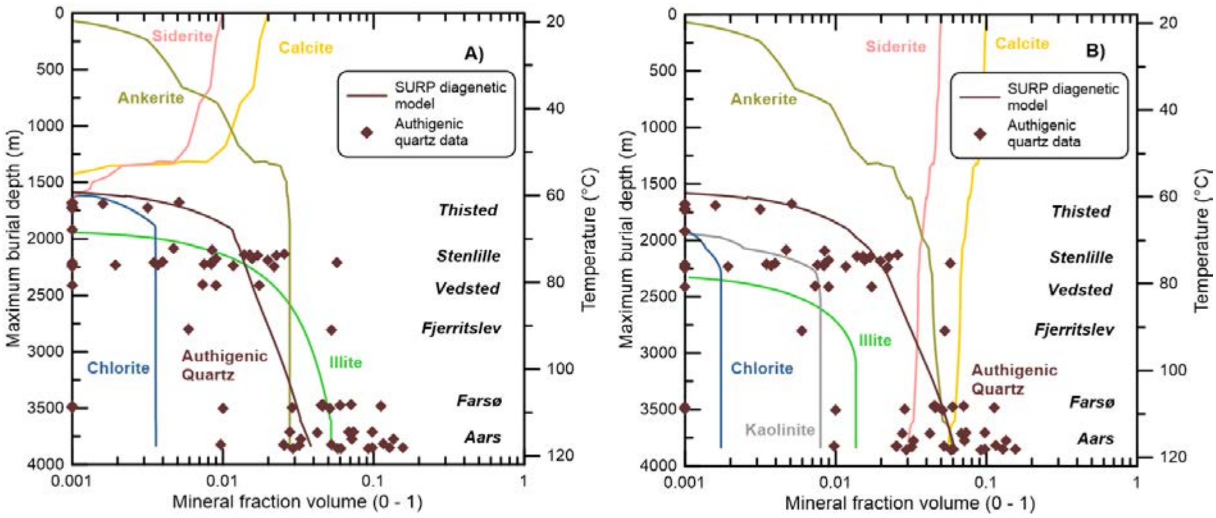

Figure 5.1: *Diagenetic evolution with depth simulated for A) in the case of excess of Mg in the formation water and B) in the case of excess of Mg in the formation water combined with an increased amount of initial carbonate minerals.*

5.2 Validation of the model

There is good agreement between the modelled and measured quartz cement volumes of the calibration and test samples and 88% of the samples are within the tolerance range of ±4% (Fig. 4.20). This shows that the burial histories for the Gassum Formation are not under- or overestimating the temperature evolution of the sandstones so the calibration of the basin modelling to the mineralogical temperature indicators has been successful.

In order to validate the Touchstone modelling, estimation of the diagenetic alterations and reservoir properties in the Farsø area is made by not including data from the Farsø-1 well in the model and then use the general knowledge about burial history and depositional setting as input together with data from the samples from the other analyzed wells. Two seismic lines pass close by the location of the Farsø-1 well and based on this information, the thickness of the Gassum Formation in the Farsø area would have been estimated to be about the same thickness as penetrated in Farsø-1. The burial history for Farsø-1 terminates with a present-day scenario with a temperature of c. 81°C, a depth of c. 2850 m, an effective stress of c. 41.3 MPa and a fluid overpressure of c. 1.2 MPa, whereas the maximum temperature and depth prior to structural inversion were c. 113°C and c. 3450 m, respectively.

Based on knowledge about the general development of depositional environments of the Gassum Formation across the basin combined with specific knowledge obtained from the local Aars-1 and Hyllebjerg-1 wells (Nielsen 2003), the petrofacies present in the Farsø area are interpreted to be primarily shoreface sandstones interbedded with lower shoreface to offshore heteroliths and mudstones. At least one thick interval of fluvial/estuarine sandstones is considered very likely to be present above the basin-wide sequence boundary 5, and additional thinner intervals of this facies and of lagoonal sandstones may also be present. Hence, separate predictions of the reservoir quality in the Farsø area are made to account for each of the petrofacies that are likely to be present. The difference between the input parameters for these scenarios is related to the knowledge obtained about ankerite cement. Furthermore, the upper limit for the grain size of the lower shoreface facies is set to 0.1 mm.

5.3 Correlation between variable characteristics

For the Touchstone simulation results obtained using the Farsø burial history, the factors that affect the variations the most based on correlation coefficients are summarized in tornado plots for the fluvial and shoreface depositional environments (Fig. 5.2). The remaining facies are not shown, but the estuarine facies can be considered equivalent to the fluvial facies, only with slightly decreased reservoir quality, and the lagoonal and lower shoreface facies are lower reservoir quality equivalents to the shoreface facies.

The permeability of both these facies is most dependent on inter-granular porosity, since high porosity between grains results in high permeability. Detrital and authigenic pore-filling clays have a negative influence on the permeability, which is most pronounced for the fluvial facies since the permeability of the shoreface facies is more dependent on ankerite cement due to its larger content in this facies. The inverse correlation between permeability and micro-porosity is caused by the high clay content present in the samples with high micro-porosity resulting in low permeability. The correlation between permeability and quartz cement is because quartz cement is most abundant in samples with low clay content resulting in a relatively smaller permeability reduction at the depths in question.

For both depositional environments, the total porosity is most dependent on the inter-granular porosity. For the fluvial deposits, the secondary porosity formed by partial dissolution of detrital grains is the second-most important influence on the total porosity, whereas the micro-porosity is the second-most important factor for the shoreface deposits, although the difference is not large. The micro-porosity is for both facies modelled to be primarily present in grains, second most in matrix and third most in cement.

Ankerite cement has the largest effect on the inter-granular porosity in the shoreface facies, whereas it has the third-largest effect in the fluvial facies after pore-filling clays. The pore-filling clay matrix has a larger influence on the inter-granular porosity than the autigenic illitic pore-fill in both fluvial and shoreface deposits, which is presumably caused by slightly smaller abundance of authigenic illite than detrital pore-fill according to the modelling results. The correlation between inter-granular porosity and quartz cement is similarly to the permeability caused by the lower clay content present in quartz-rich samples, which tend to have the highest permeabilities.

Grain coating causes the largest reduction in quartz cement formation in the fluvial facies, whereas its influence is secondary to ankerite in the shoreface facies. Pore-filling detrital clays also hinder the quartz precipitation as well as authigenic illite. The abundance of monocrystalline quartz has a strong correlation to the amount of quartz cement that can form.

Ankerite cement does not affect porosity and permeability significantly when it is present in contents smaller than 5% as in the fluvial facies. The correlation between quartz cement and both permeability and inter-granular porosity, signifying that quartz cement is most abundant in clay-poor lithologies, is enhanced when more ankerite cement is present. This is because the formation of ankerite decreases the influence of the detrital and authigenic clays on the reservoir properties and results in smaller abundances of quartz cement. The large volumes of ankerite cement in the shoreface facies decrease the effect of clays on reservoir properties since ankerite is the main control on the reduction of permeability and inter-granular porosity.

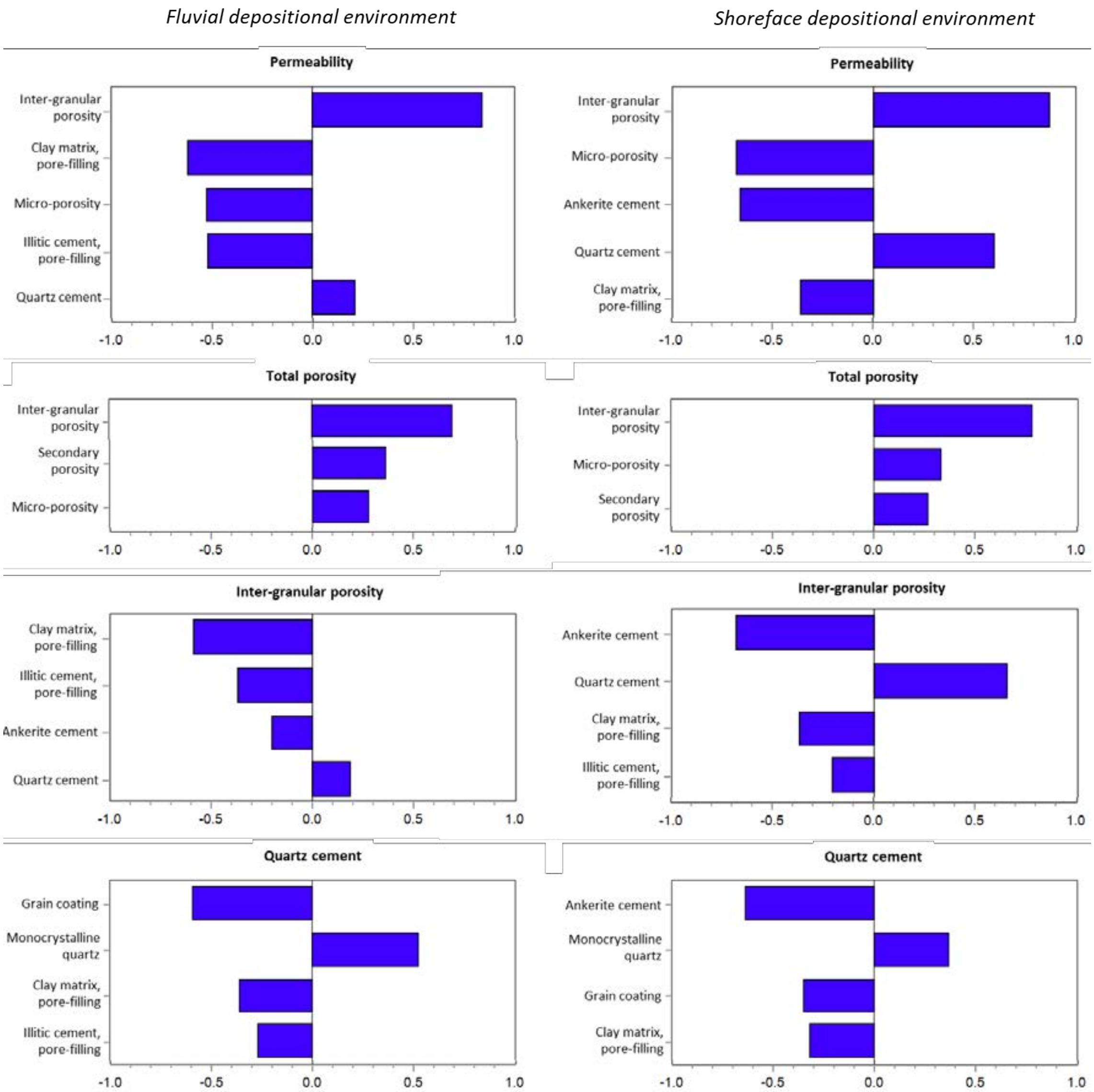

Figure 5.2: *Tornado plots showing which factors affect permeability, total porosity, inter-granular porosity and quartz cement formation the most according to the simulation results for fluvial and shoreface deposits in the Farsø area.*

5.4 Estimation of reservoir quality

The simulation results for Gassum Formation in the Farsø area is based on 1000 realizations of each facies employing the available data from other wells and selected results are shown in Table 5.1. The modelled porosity and permeability developments with time for the Farsø area are shown in Figure 5.3 for the shoreface facies since this is the dominant petrofacies. Aside from the initial compaction following deposition, the largest reduction in reservoir properties occurred simultaneously with the deepest burial of the formation. The P50 estimate refers to the value that is exceeded by 50% of the estimates in the simulation results, and the P10 and P90 estimates are the highest and lowest, respectively, of the reported estimates. The P50 estimate of the present-day porosity and permeability is 11.6% and 8.3 mD, respectively, for the shoreface facies.

The simulated values of ankerite and quartz cement volumes, porosity and permeability for the shoreface facies in the Farsø area are shown in Figure 5.4 together with the actual results from 12 analyses of core material from the Farsø-1 well. The calculated values correlate well with the measured values, although there is a trend of underestimating the occurrence of the highest and lowest values. This trend is especially pronounced for the ankerite cement, whereas all measured values of quartz cement value and reservoir properties are within the estimated range.

The simulated results for the fluvial and shoreface facies are compared considering the reservoir properties in Figure 5.5 and the cement volumes in Figure 5.6. The major difference between these facies is related to the much higher intergranular porosity in the fluvial sandstones caused by the lower amount of ankerite precipitation and resulting in higher permeability. The simulated mean values for ankerite cement are 2.52% for fluvial sandstones and 9.05% for shoreface sandstones (Table 5.1). Therefore, even though the difference in total porosity between these facies is only 3%, still the effect on the reservoir quality is large. The ankerite precipitation results in less quartz cement formation and a little less illitic cement.

The results of the prediction modelling for the Gassum Formation in the Farsø area show that the reservoir quality is not good enough for geothermal energy exploitation in this area, which is in agreement with the measured values from the Farsø-1 well (Fig. 5.4). This is because the diagenesis is very advanced due to the deep burial of the formation in this area resulting in rather low porosity and permeability. However, only shoreface facies sandstones have been cored in the well, but the sequence stratigraphic interpretation shows that fluvial/estuarine sandstones are also present in the formation in this area and the modelling results show that these sandstones presumably have better reservoir quality than the shoreface sandstones (Fig. 5.5).

The simulated trends in reservoir properties between the different depositional environments are supposedly similar at shallower depths, but with better reservoir quality due to less advanced diagenesis. Hence, the intervals with fluvial sandstones are expected to have the best reservoir quality in each new well, except perhaps for the special case where chlorite coatings have helped preserve good reservoir quality in in estuarine and shoreface sandstones deposited at forced regressive conditions (Weibel et al. 2017a). The reservoir quality of the lower shoreface to offshore facies is not expected to be as much better as the other facies at shallower depths since the high micro-porosity and the heterolithic nature will still result in low permeability.

Table 5.1: *Mean values of the modelling results for the Farsø area for five different depositional environments that are considered possible to be present.*

Depositional environment	*Fluvial*	*Estuarine*	*Lagoonal*	*Shoreface*	*Lower shoreface*
Permeability (mD)	*237.55*	*147.02*	*12.32*	*88.11*	*10.61*
Total porosity (%)	*14.93*	*13.68*	*9.66*	*11.71*	*11.20*
Inter-granular porosity (%)	*7.92*	*6.71*	*2.82*	*4.80*	*4.75*
Inter-granular volume IGV (%)	*24.74*	*25.22*	*26.43*	*25.80*	*30.64*
Quartz overgrowth thickness (µm)	*15.4*	*15.2*	*12.2*	*12.8*	*3.3*
Quartz nucleation surface area (mm²)	*38.1*	*34.1*	*18.7*	*26.1*	*48.5*
Quartz cement (%)	*7.44*	*6.69*	*3.95*	*5.25*	*4.17*
Ankerite cement (%)	*2.52*	*5.02*	*13.05*	*9.05*	*15.48*
Illitic pore-filling cement (%)	*1.33*	*1.30*	*1.20*	*1.23*	*1.17*
Chloritic pore-lining cement (%)	*0.07*	*0.07*	*0.07*	*0.07*	*0.06*
Kaolinitic cement (%)	*0.34*	*0.33*	*0.33*	*0.33*	*0.31*

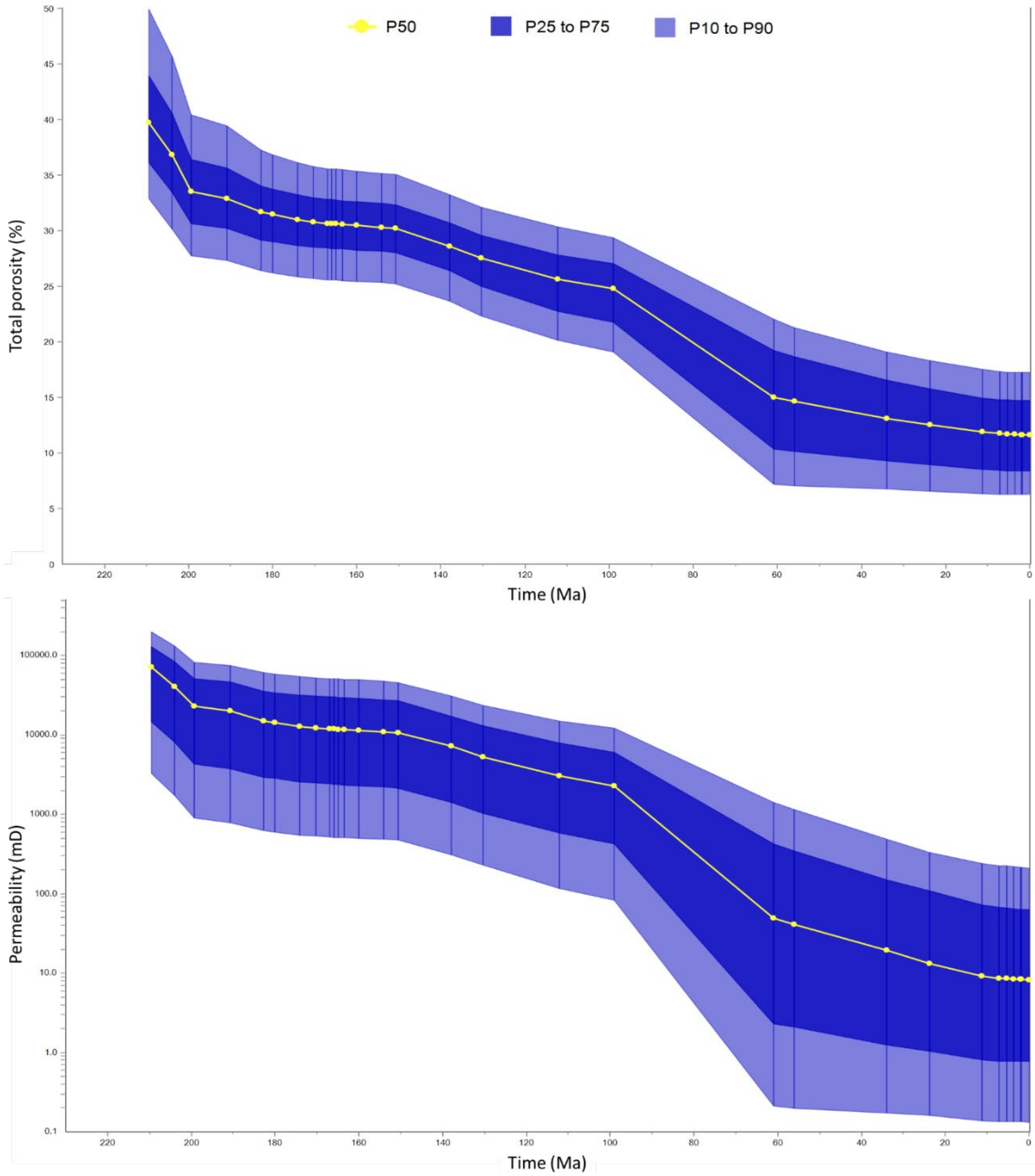

Figure 5.3: *Porosity and permeability development with time for the shoreface depositional environment in the Farsø area modelled with Touchstone.*

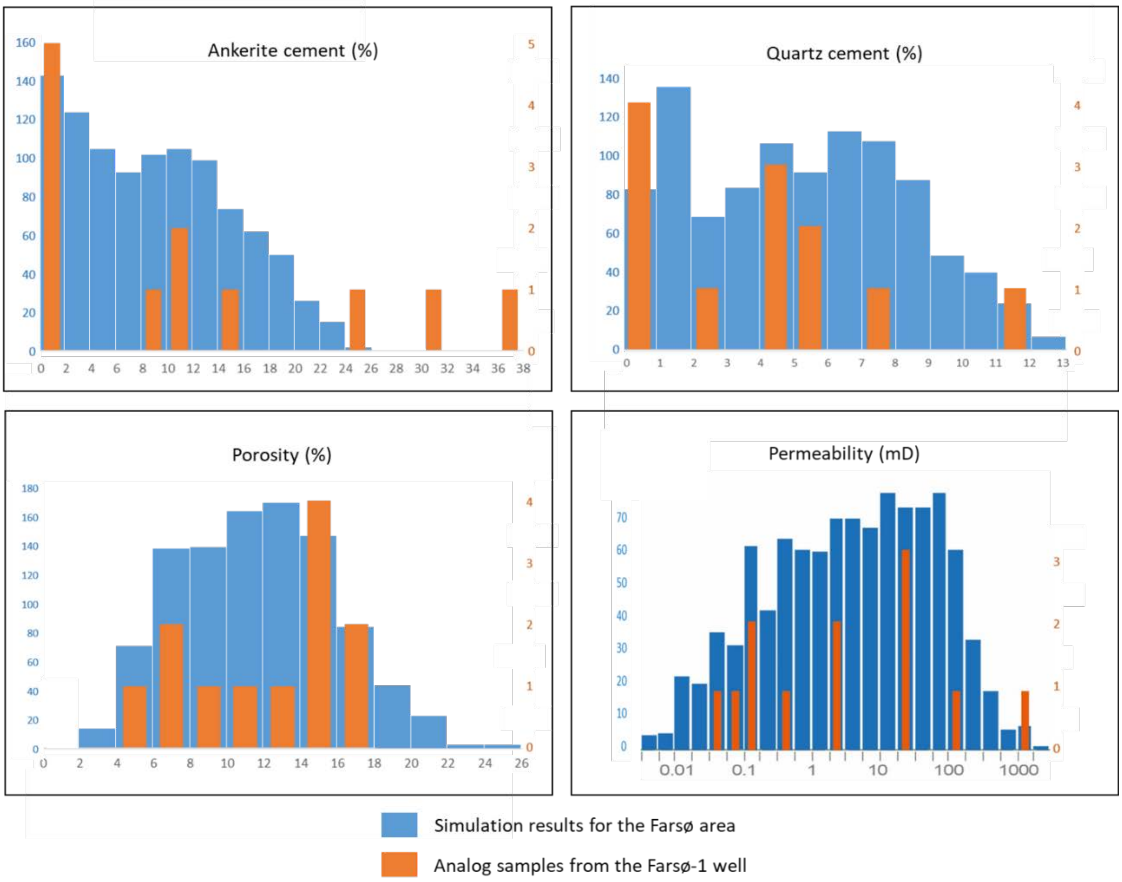

Figure 5.4: *The simulation results for Gassum Formation in the Farsø area is based on 1000 realizations of the shoreface facies employing the available data from other wells. The actual results from 12 analyses of core material from the Farsø-1 well is shown for comparison.*

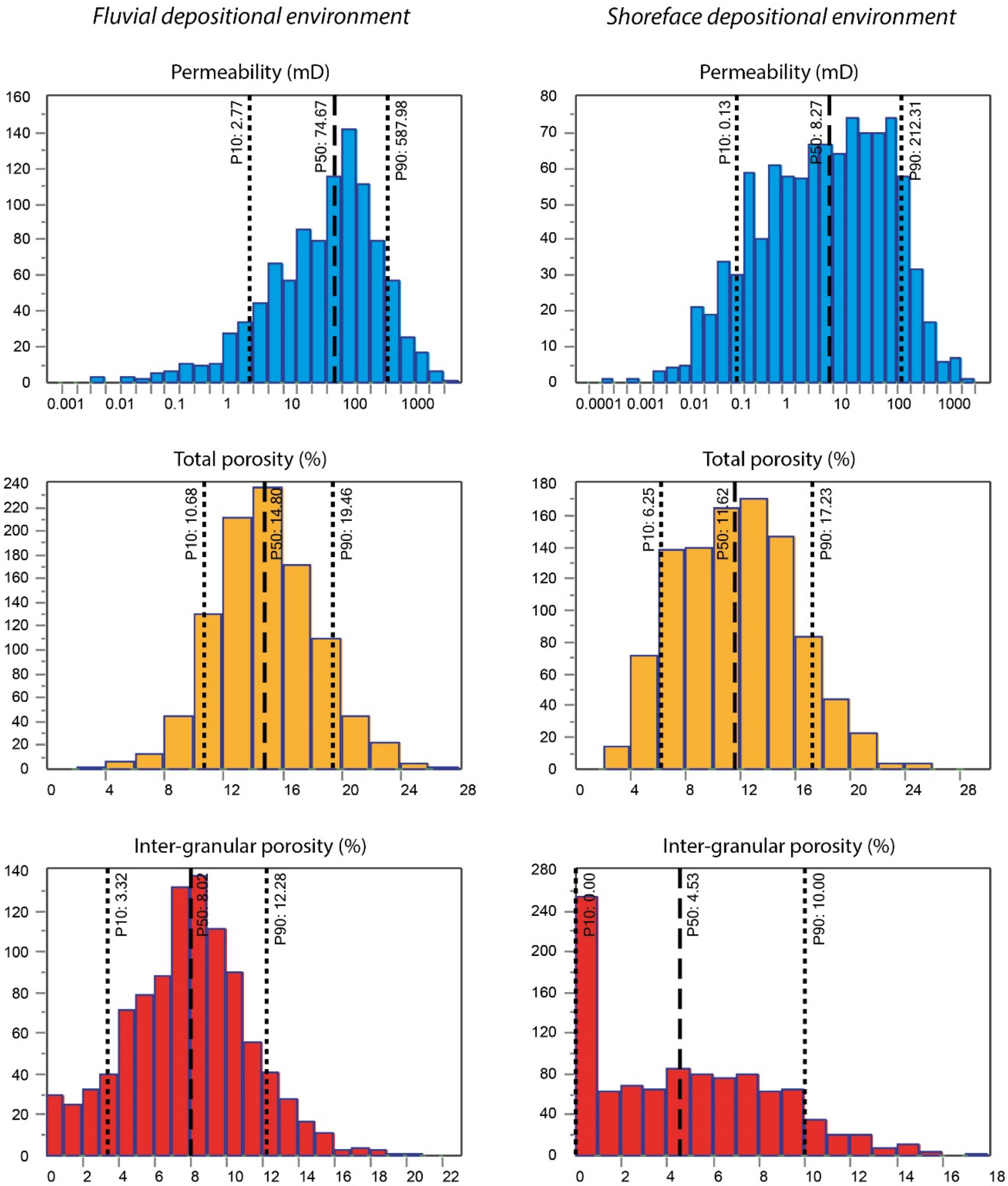

Figure 5.5: *Comparison of simulation results of reservoir properties in the Farsø area for fluvial and shoreface facies. The P10, P50 and P90 values indicate the modelled tenth, fiftieth and ninetieth percentile of the 1000 realizations.*

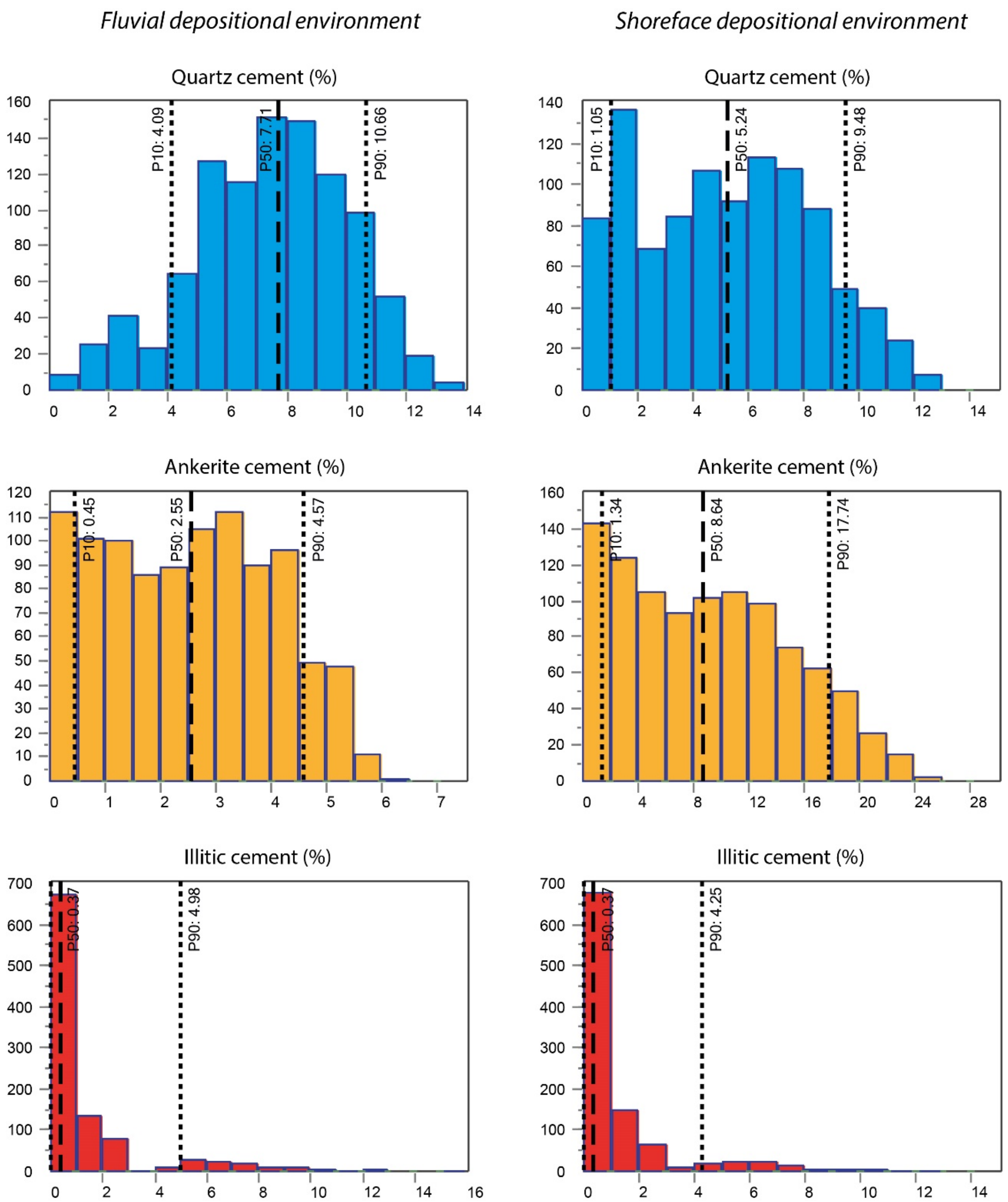

Figure 5.6: *Comparison of simulation results of selected cement types in the Farsø area for fluvial and shoreface facies. The P10, P50 and P90 values indicate the modelled tenth, fiftieth and ninetieth percentile of the 1000 realizations.*

6. Conclusions

- The diagenesis modelling has proven suitable for estimating the influence of compaction and diagenesis on the reservoir properties, hence validating the applicability.
- The thermodynamic modelling results made by SURP give important insights about the conditions for carbonate mineral dissolution and precipitation, which can be critical for the reservoir quality.
- Pore-filling ankerite cement can only form when there is enough Mg available in the pore water and when a precursor carbonate mineral is present, and the largest amounts of ankerite can precipitate when both calcite and siderite are dissolving. The availability of Ca in the pore water is also necessary for the ankerite formation, whereas Fe is in excess in the system.
- The temperature constraints obtained by combining data of vitrinite reflectance, fluid inclusions in quartz cement and oxygen isotopes in carbonate cement give comparable results that are successfully used to calibrate the basin modelling made by PetroMod.
- The stressed porosity and permeability results show that the porosity decreases only slightly when exposing the samples to reservoir pressure, whereas the fluid permeability is reduced to about two-thirds.
- The obtained data and knowledge of petrographic compositions, reservoir properties, depositional environments, burial histories and mineralogical reactions are integrated in the Touchstone modelling, thereby establishing a robust model for estimation of geothermal reservoir quality of the Gassum Formation.
- Testing and optimization of the model parameters made it possible to calculate cement volumes and reservoir properties with an acceptable fit to the measured values. Validation of the model could then be made by estimating the same parameters for a chosen area and then comparing with analog samples, which gives a good match.
- The sensitivity of the reservoir properties to variations in cement type and amount is for example evident for the inter-granular porosity that is much reduced by pervasive cementation although the total porosity is still rather high due to micro-porosity, whereas the permeability is much affected.
- The mineralogical composition and grain size of the deposited sediment is related to which depositional environment it belongs to, and this variability affects the subsequent diagenesis such that the reservoir quality evolves differently for the different facies. Therefore, a model scenario for each depositional facies is necessary for obtaining a detailed estimate.
- Thus, the reservoir quality may be very varied within the formation at a given well location, such as for the Farsø area where some of un-cored

intervals are estimated to have better reservoir quality than the cored and analyzed succession.

Further studies

The diagenesis model that has been established for the Gassum Formation in GEOTHERM can be used to make qualified pre-drill estimates of reservoir properties if local and regional variations are thoroughly considered. Similarly, the establishment of a diagenesis model for the Skagerrak/Bunter Formation would give important insights about where this reservoir has properties that are appropriate for geothermal energy exploitation; therefore, the creation of such a model is recommended.

The results of the diagenesis modelling including reservoir quality prediction by Touchstone software at potential well locations can be extended onto map surfaces using T>Map software by incorporating 3D basin modelling, burial histories and facies distributions. In this way, the spatial distribution of the reservoir properties can be simulated for an entire sandstone reservoir along each of its prominent surfaces, by taking the temperature- and facies-dependence of the different diagenetic processes into account. This approach is recommended for future studies.

Acknowledgements

The Innovation Fund Denmark is acknowledged for funding the project GEO-THERM, thereby making the diagenesis modelling possible. The authors would like to thank Robert H. Lander and Linda M. Bonnell for assistance with the Touchstone modelling; Martin J. Whitehouse, Lev S. Ilyinsky and Kerstin Lindén for help at the SIMS facility; Tod Waight for help with the microprobe; Hans J. Lorentzen for performing core analyses.

References

Aagaard, P., Egeberg, P.K., Saigal, G.C., Morad, S., Bjørlykke, K., 1990. Diagenetic albitization of detrital K-feldspars in Jurassic, Lower Cretaceous and Tertiary clastic reservoir rocks from offshore Norway, II. Formation water chemistry and kinetic considerations. Journal of Sedimentary Petrology 60, 575–581.

Ajdukiewicz, J.M., Nicholson, P.H., Esch, W.L., 2010. Prediction of deep reservoir quality using early diagenetic process models in the Jurassic Norphlet Formation, Gulf of Mexico. AAPG Bulletin 94, 1189–1227.

American Petroleum Institute, 1998. API RP 40, Recommended Practice for Core Analysis, second edition. American Petroleum Institute, Washington DC.

Beaufort, D., Cassagnabere, A., Petit, S., Lanson, B., Berger, G., Lacharpagne, J.C., Johansen, H., 1998. Kaolinite-to-dickite reaction in sandstone reservoirs. Clay Minerals 33, 297–316.

Bjørlykke, K., 2010. Petroleum Geoscience: From Sedimentary Environments to Rock Physics. Springer, 508 pp.

Busch, B., Hilgers, C., Lander, R.H., Bonnell, L.M., Adelmann, D., 2018. Reservoir quality and burial model evaluation by kinetic quartz and illite cementation modeling: Case study of Rotliegendes, north Germany. AAPG Bulletin 102, 293–307.

Charlton, S.R., Parkhurst, D. L., 2011. Modules based on the geochemical model PHREEQC for use in scripting and programming languages. Computers & Geosciences 37, 1653–1663.

Cui, Y., Jones, S.J., Saville, C., Stricker, S., Wang, G., Tang, L., Fan, X., Chen, J., 2017. The role played by carbonate cementation in controlling reservoir quality of the Triassic Skagerrak Formation, Norway. Marine and Petroleum Geology 85, 316–331.

English, K.L., English, J.M., Bonnell, L.M., Lander, R.H., Hollis, C., Redfern, J., Guirdham, C., Garnham, J., Cherif, R.Y., 2017. Controls on reservoir quality in exhumed basins – an example from the Ordovician sandstone, Illizi Basin, Algeria. Marine and Petroleum Geology 80, 203–227.

Fuchs, S., Balling, N., Mathiesen, A., 2020. Deep basin temperature and heat-flow field in Denmark – New insights from borehole analysis and 3D geothermal modelling. Geothermics 83, 101722.

Holmslykke, H.D., Schovsbo, N.H., Kristensen, L., Weibel, R., Nielsen, L.H., 2019. Characterising brines in deep Mesozoic sandstone reservoirs, Denmark. Geological Survey of Denmark and Greenland Bulletin 43, e2019430104.

Horibe, Y., Oba, T., 1972. Temperatures scales of aragonite–water and calcite–water systems. Fossils 23/24, 69–70 (in Japanese).

Japsen, P., Bidstrup, T., 1999. Quantification of late Cenozoic erosion in Denmark based on sonic data and basin modelling. Bulletin of Geological Society of Denmark 46, 79–99.

Japsen, P., Green, P.F., Nielsen, L.H., Rasmussen, E.S., Bidstrup, T., 2007. Mesozoic-Cenozoic exhumation events in the eastern North Sea Basin: a multi-disciplinary study based on palaeothermal, palaeoburial, stratigraphic and seismic data. Basin Research 19, 451–490.

Kristensen, L., Hjuler, M.L., Frykman, P., Olivarius, M., Weibel, R., Nielsen, L.H., Mathiesen, A., 2016. Pre-drilling assessments of average porosity and permeability in geothermal reservoirs of the Danish area. Geothermal Energy 4(6), 27p.

Magoon, L.B., Dow, W.G., 1994. The petroleum system, in L.B. Magoon and W.G. Dow, eds., The Petroleum System – From Source to Trap: American Association of Petroleum Geologists Memoir 60, 3–24.

Mansurbeg, H., Morad, S., Salem, A., Marfil, R., El-ghali, M.A.K., Nystuen, J.P., Caja, M.A., Amorosi, A., Garcia, D., La Iglesia, A., 2008. Diagenesis and reservoir quality evolution of palaeocene deep-water, marine sandstones, the Shetland-Faroes Basin, British continental shelf. Marine and Petroleum Geology 25, 514–543.

Mathiesen, A., Nielsen, L.H., Bidstrup, T., 2010. Identifying potential geothermal reservoirs in Denmark. Geological Survey of Denmark and Greenland Bulletin 20, 19–22.

McBride, E.F., 1963. A classification of common sandstones. Journal of Sedimentary Research 33, 664–669.

Michelsen, O., Clausen, O.R., 2002. Detailed stratigraphic subdivision and regional correlation of the southern Danish Triassic succession. Marine and Petroleum Geology 19, 563–587.

Michelsen, O., Nielsen, L.H., Johannessen, P.N., Andsbjerg, J., Surlyk, F., 2003. Jurassic lithostratigraphy and stratigraphic development onshore and offshore Denmark. Geological Survey of Denmark and Greenland Bulletin 1, 147–216.

Nielsen, S.B., Clausen, O.R., McGregor, E., 2015. Basin%Ro: A vitrinite reflectance model derived from basin and laboratory data. Basin Research 29, 515–536.

Nielsen, L.H., 2003. Late Triassic – Jurassic development of the Danish Basin and the Fennoscandian Border Zone, southern Scandinavia. Geological Survey of Denmark and Greenland Bulletin 1, 459–526.

Poulsen, S.E., Balling, N., Bording, T.S., Mathiesen, A., Nielsen, S.B., 2017. Inverse geothermal modelling applied to Danish sedimentary basins. Geophysical Journal International 211, 188–206.

Sliwinski, M.G., Kitajima, K., Kozdon, R., Spicuzza, M.J., Fournelle, J.H., Denny, A., Valley, J.W., 2015. Secondary ion mass spectrometry bias on isotope ratios in dolomite–ankerite, Part I: δ18O matrix effects. Geostandards and Geoanalytical Research 40, 157–172.

Sweeny, R.E., Burnham, A.K., 1990. Evaluation of a simple model of vitrinite reflectance based on chemical kinetics. American Association of Petroleum Geologists Bulletin 74, 1559–1570.

Taylor, T.R., Giles, M.R., Hathon, L.A., Diggs, T.N., Braunsdorf, N.R., Birbiglia, G.V., Kittridge, M.G., Macaulay, C.I., Espejo, I.S., 2010. Sandstone diagenesis and reservoir quality predictions: models, myths, and reality. AAPG Bulletin 94, 1093–1132.

Taylor, T.R., Kittridge, M.G., Winefield, P., Bryndzia, L.T., Bonnell, L.M., 2015. Reservoir quality and rock properties modeling e Triassic and Jurassic sandstones, greater Shearwater area, UK Central North Sea. Marine and Petroleum Geology 65, 1–21.

Tobin, R.C., McClain, T., Lieber, R.B., Ozkan, A., Banfield, L.A., Marchand, A.M.E., McRae, L.E., 2010. Reservoir quality modeling of tight-gas sands in Wamsutter field: Integration of diagenesis, petroleum systems, and production data. AAPG Bulletin 94, 1229–1266.

Tremosa, J., Gailhanou, H., Chiaberge, C., Castilla, R., Gaucher E.C., Lassin, A., Gout, C., Fialips, C., Claret, F., 2020. Effects of smectite dehydration and illitisation on overpressures in sedimentary basins: a coupled chemical and thermo-hydro-mechanical modelling approach. Marine and Petroleum Geology 111, 166–178.

Vejbæk, O.V., 1997. Dybe strukturer i danske sedimentære bassiner. Geologisk Tidsskrift 4, 1–31.

Vosgerau, H., Mathiesen, A., Andersen, M.S., Boldreel, L.O., Hjuler, M.L., Kamla, E., Kristensen, L., Pedersen, C.B., Pjetursson, B., Nielsen, L.H., 2016. A WebGIS portal for exploration of deep geothermal energy based on geological and geophysical data. Geological Survey of Denmark and Greenland Bulletin 35, 23–26.

Weibel, R., Olivarius, M., Kristensen, L., Friis, H., Hjuler, M.L., Kjøller, C., Mathiesen, A., Nielsen, L.H., 2017a. Predicting permeability of low-enthalpy geothermal reservoirs: Acase study from the Upper Triassic – Lower Jurassic Gassum Formation, Norwegian–Danish Basin. Geothermics 65, 135–157.

Weibel, R., Olivarius, M., Kjøller, C., Kristensen, L., Hjuler, M.L., Friis, H., Pedersen, P.K., Boyce, A., Andersen, M.S., Kamla, E., Boldreel, L.O., Mathiesen, A., Nielsen, L.H., 2017b. The influence of climate on early and burial diagenesis of Triassic and Jurassic sandstones from the Norwegian–Danish Basin. The Depositional Record 3(1), 60–91.

Worden, R.H., Armitage, P.J., Butcher, A.R., Churchill, J.M., Csoma, A.E., Hollis, C., Lander, R.H., Omma, J.E., 2018. Petroleum reservoir quality prediction: overview and contrasting approaches from sandstone and carbonate communities. Geological Society, London, Special Publications 435, 1–31.

Wygrala, B.P., 1989. Integrated study of an oil field in the Southern Po Basin, Northern Italy. Ph.D. dissertation, University of Cologne, 217 p.

Zheng, Y.-F., 1999. Oxygen isotope fractionation in carbonate and sulfate minerals. Geochemical Journal 33, 109–126.